

Concomitant memantine and *Lactobacillus plantarum* treatment attenuates cognitive impairments in APP/PS1 mice

Qiu-Jun Wang^{1,*}, Yue-E Shen^{2,*}, Xin Wang³, Shuang Fu³, Xin Zhang³, Yi-Na Zhang⁴, Rui-Tao Wang³

¹General Practice Department, The Second Affiliated Hospital, Harbin Medical University, Harbin 150086, China

²Department of Neurology, The First Affiliated Hospital of Harbin Medical University, Harbin 150001, China

³Department of Internal Medicine, Harbin Medical University Cancer Hospital, Harbin Medical University, Harbin 150081, China

⁴Department of Geriatrics, The Second Affiliated Hospital, Harbin Medical University, Harbin 150086, China

*Equal contribution

Correspondence to: Yi-Na Zhang Rui-Tao Wang; email: zhangyina2000@yahoo.cn, ruitaowang@126.com

Keywords: Alzheimer's disease, APP/PS1 mice, trimethylamine-N-oxide, cognitive behavior, *L. plantarum*

Received: November 6, 2019

Accepted: December 23, 2019

Published: January 6, 2020

Copyright: Wang et al. This is an open-access article distributed under the terms of the Creative Commons Attribution License (CC BY 3.0), which permits unrestricted use, distribution, and reproduction in any medium, provided the original author and source are credited.

ABSTRACT

Trimethylamine-N-oxide (TMAO) is a gut microbial metabolite that promotes Alzheimer's disease (AD) progression. Given that probiotics can alleviate AD symptoms by inhibiting the synthesis of TMAO, here we investigated the correlation between TMAO and cognitive deterioration by measuring TMAO levels in the plasma of choline-treated APP/PS1 mice (an AD mouse model) with and without probiotic treatments. We found that declines in *L. plantarum* in the gut were associated with cognitive impairment. Moreover, 12-weeks of treatment with memantine plus *L. plantarum* ameliorated cognitive deterioration, decreased A β levels in the hippocampus, and protected neuronal integrity and plasticity. These effects were accompanied by reductions in TMAO synthesis and neuroinflammation. These experiments demonstrate that *L. plantarum* augments the beneficial therapeutic effects of memantine treatment in APP/PS1 mice by remodeling the intestinal microbiota, inhibiting the synthesis of TMAO, and reducing clusterin levels. Our results thus highlight intestinal microbiota as a potential therapeutic target to decrease the risk of AD.

INTRODUCTION

The rising longevity of humans will increase the incidence of dementias such as Alzheimer's disease (AD) [1]. Increased levels of extracellular amyloid- β (A β) peptide in neuritic plaques and intracellular fibrillar aggregates of phosphorylated tau are pathological hallmarks of AD in brain tissues, in addition to the widespread loss of neurons and synapses [2]. The underlying pathogeny of AD is highly complex and polyfactorial, including contributions from gut microbiota among other genetic and environmental factors [3, 4]. Elevated levels of the trimethylamine N-oxide (TMAO) metabolite are strongly associated with AD pathology [5]. Additionally, TMAO levels are

elevated in cerebrospinal fluid (CSF) from AD patients compared to cognitively-unimpaired individuals and serve as an AD biomarker [6].

TMAO influences cholesterol and sterol metabolism and increased levels of it correlate with adverse cardiovascular outcomes [7]. TMAO is a gut microbial metabolite of dietary meat and fat. In the gut, unabsorbed carnitine is converted by intestinal microbiota into trimethylamine (TMA). Thereafter, TMA is oxidized to TMAO by flavin monooxygenase (FMO) in the liver [8]. By virtue of this, the intestinal flora is a major modulator of TMAO-induced diseases and thus constitutes a new potential therapeutic target [9]. Suppression of intestinal microbiota with oral

broad-spectrum antibiotics attenuated TMAO-caused atherosclerosis by reducing TMAO synthesis [8]. Nevertheless, treatment with broad-spectrum antibiotics is limited due to side effects and the possibility of antibiotic resistance. Hence, the identification of probiotics with excellent modulatory effects on the composition of the gut microbiome to inhibit TMA production might be useful for the prevention and treatment of AD.

Probiotics are defined as live microorganisms which, when administered or ingested in adequate amounts, confer a health benefit to the host. The contribution of intestinal microbiota to cognitive decline can be indirectly measured by the effects of probiotic supplementation on AD. Supplementation with probiotics ameliorated AD symptoms and improved biochemical markers in human patients [10] and animal models [11].

The mechanisms whereby TMAO contributes to pathological processes in AD have not been fully investigated. Therefore, in this study, we examined cognitive functions, TMAO synthesis, and the composition of the intestinal microflora in choline-treated mice. We also used the PROBIO database to predict the probiotics most likely to modify TMA/TMAO levels in plasma and behavioral symptoms. To test the effects of *Lactobacillus plantarum* (*L. plantarum*) on AD, we investigated the effects of *L. plantarum* and memantine in combination with *L. plantarum* on cognitive impairment, long-term potentiation (LTP), pathological deterioration, and TMAO synthesis in male transgenic AD mice. Lastly, we assessed the ability of *L. plantarum* alone or in combination with memantine to elicit the release of clusterin in plasma and relieve inflammation in the hippocampus.

RESULTS

Effects of choline supplementation on cognitive declines in C57BL/6J mice

Choline supplementation ameliorates specific behavioral, neurological, and cognitive deficits [12]. However, higher choline intake is associated with poorer brain health and cognitive function among adults [13]. In our study here, the locomotor activity of C57BL/6J mice was the same as that of choline-treated mice (Figure 1A). In the nest building test, the mean score of the choline-treated group was lower than that of the C57BL/6J group (Figure 1B). To assess novel object recognition memory in these mice, we utilized the novel object recognition test (Figure 1C, 1D). Administration of choline caused a decline in short-term memory but had no effect on long-term object recognition. To examine spatial learning and memory in mice, we subjected them to the Morris water maze test

(Figure 1E, 1F). In the training session, choline-treated mice exhibited a longer escape latency than C57BL/6J mice beginning on the third day. In the testing session, the swimming time within the target quadrant was lower for choline-treated mice than for C57BL/6J mice; however, there was no difference in the number of plate crossings, and swimming speed (data not shown) between the control group and choline-treated group. Finally, we subjected the mice to the shuttle-box test to evaluate their active avoidance (Figure 1G, 1H). Successful avoidance times were lower for the choline-treated group than for the control group beginning on the sixth day in the training phase as well as in the testing phase. These data indicated that learning and memory declined in C57BL/6J mice with long-term 1% choline administration.

Effects of choline supplementation on TMAO synthesis in C57BL/6J mice

To investigate the effect of choline supplementation on TMAO synthesis in C57BL/6J mice, we measured TMA and TMAO levels in plasma at three months after administration. Using liquid chromatography-tandem mass spectrometry (LC/MS), we found that plasma TMA and TMAO levels were much higher in choline-treated mice than those in the control group (Figure 2). Our results suggested that long-term choline supplementation increased TMAO synthesis levels in C57BL/6J mice.

Correlation analysis of cognitive declines and reduced TMAO synthesis in choline-treated C57BL/6J mice

To further assess the correlations between altered plasma TMA/TMAO and cognitive declines in choline-treated C57BL/6J mice, we first analyzed the experimental results of nest building test, novel object recognition test, Morris water maze test, and shuttle-box test using principal component analysis (PCA). PCA revealed principal components 1 (PC1, 89.78%) and 2 (PC2, 6.58%), which grouped mice into two distinct clusters (Figure 3A). The average of PCA scores across the aforementioned tests constitutes the global behavioral index of mice in our study. This index shows that the behavioral characteristics of choline-treated mice differed from those of C57BL/6J mice (Figure 3B). Subsequently, to test the discriminatory power of plasma TMA and TMAO levels in properly classifying mice groups, we calculated the average area under the ROC (Figure 3C). We noticed that the area under the curve (AUC) for each group was 0.6189 for TMA levels and 0.7333 for TMAO levels. AUC values <0.7 implies that the corresponding indicator is not a good metric to classify the study groups [14]. Spearman correlation

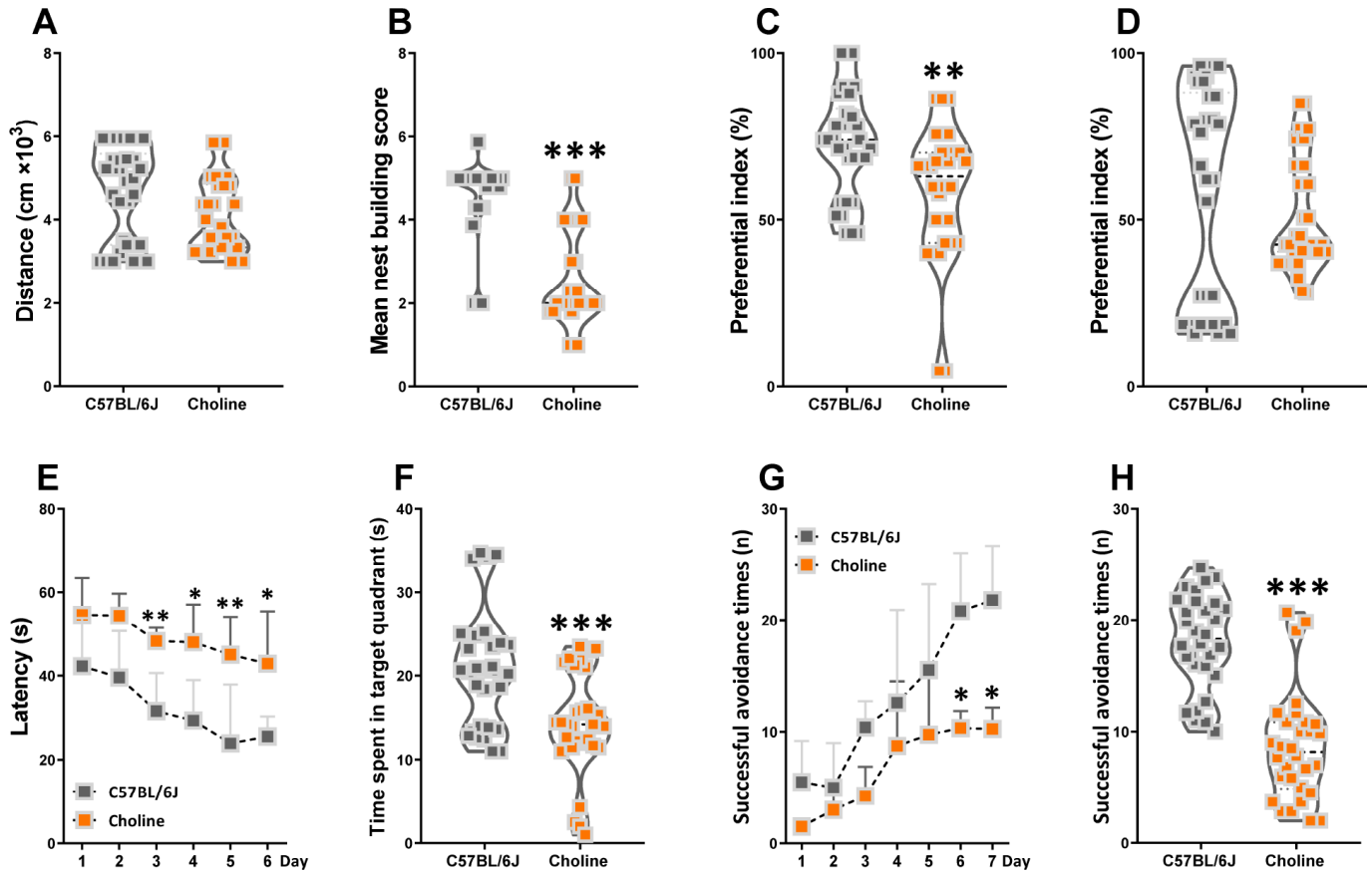


Figure 1. Effects of choline supplementation on cognitive declines in C57BL/6J mice. The spontaneous locomotor activity (A), nest building score (B), preferential index after training 1 hour (C) and 24 hours (D) in the phase of novel object test, latency in the learning phase (E) and time spent in target quadrant in the testing phase (F) of Morris water maze test, successful avoidance times in the learning (G) and testing phase (H) of shuttle box test. * $P < 0.05$, ** $P < 0.01$, *** $P < 0.001$, versus the C57BL/6J mice, by unpaired Student's t -tests. All values are mean \pm S.D. $n = 30$.

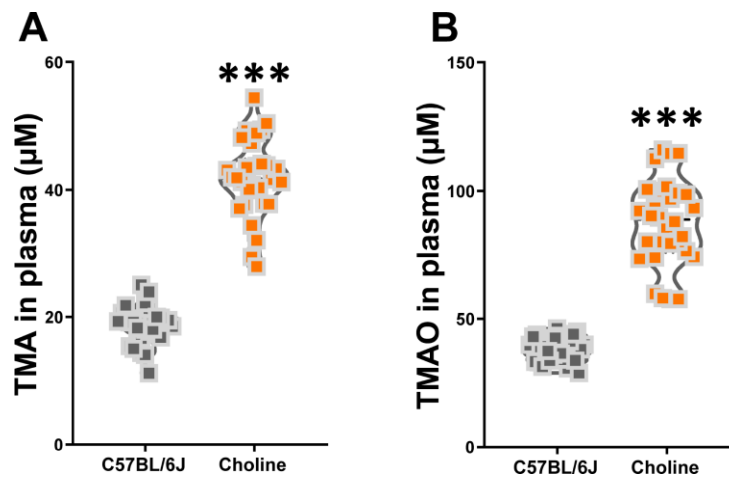


Figure 2. Effects of choline supplementation on TMAO synthesis in C57BL/6J mice. Plasma TMA (A) and TMAO (B) levels in C57BL/6J mice with or without choline supplementation (1%) as determined by LC/MS. *** $P < 0.001$, versus the C57BL/6J mice, by unpaired Student's t -tests. All values are mean \pm S.D. $n = 30$.

analyses showed that between the circulating TMA, TMAO levels, and global index of cognitive profile in WT and APP/PS1 mice. TMAO levels were correlated with the global index of cognitive profile (Figure 3D). These results indicated that increased plasma TMAO levels are associated with cognitive declines in C57BL/6J mice.

Effects of choline supplementation on microbial remodeling in C57BL/6J mice

The generation of circulating TMAO in plasma is dependent on intestinal microflora that can metabolize dietary choline into TMA, which is then converted into TMAO by members of the FMO family in the liver, among which FMO3 has been shown to be the most active enzyme [60]. Thus, to clarify the role of the intestinal microbiota in the choline-induced increase of TMAO levels, we investigated intestinal microbial populations in the gut at the phylum and species levels by metagenomic analyses. Analysis at the phylum level showed that the bacterial population of vehicle-treated C57BL/6J mice was dominated by *Bacteroidetes* (50.9%) and *Firmicutes* (40.5%), with a low level of *Proteobacteria* (4.6%) (Figure 4A). The relative amount of sequences assigned to *Firmicutes* was increased in metagenomes of choline-fed C57BL/6J mice at the expense of *Bacteroidetes* (Figure 4A). Species-level analysis revealed that choline induced a decrease in the relative abundances of *Clostridium_sp_CAG_1024*, *Psychrobacter_lutiphocae*, *Lactobacillus_saniviri*, *Eubacterium_sp_CAG_86*, *Citromicrobium_sp_WPS32*, *Candidatus_Arsenophonus_triatominarum*, *Herbinix_hemicellulosilytica*, *Halomonas_smyrnensis*, *Shewanella_algae*, *Eubacterium_siraeum*, *Burkholderia_anthina*, *Acidaminococcus_sp_CAG_917* (Figure 4B and 4F). Choline administration resulted in an increase in

the relative abundances of *Parabacteroides_johnsonii*, *Alloprevotella_rava*, *Parabacteroides_merdae*, *Bacteroides_sartorii*, *Prevotella_sp_CAG_755*, *Prevotella_sp_CAG_891*, *Bacteroides_massiliensis*, *Prevotella_sp_CAG_5226*, *Bacteroides_uniformis*, *Lactobacillus_plantarum*, *unclassified_g_Bacteroides* (Figure 4B and 4F). We used PCA to determine the influences of choline on intestinal microbial populations in the gut at the species levels. The PC1 and PC2 grouped mice from the different groups into two distinct clusters (Figure 4C). The overall gut microbiota of choline-fed C57BL/6J mice, standardized for their performance, is presented in Figure 4D. The index clearly shows that the intestinal microbial characteristics of choline-treated mice differed from that of C57BL/6J mice. Spearman correlation analyses revealed that, at the species level, there were eight bacterial species correlated with cognitive abilities, including one negatively correlated (*Odoribacter_sp_CAG_788*) and one positively correlated (*Rikenella_microfusus*) with object recognition memory, three negatively correlated (*Bacteroides_sartorii*, *Parabacteroides_merdae* and *Parabacteroides_goldsteinii*) and two positively correlated (*Lactobacillus_plantarum* and *Firmicutes_bacterium_CAG_475*) with spatial learning and memory, and two negatively correlated (*Odoribacter_sp_CAG_788* and *Parabacteroides_merdae*) and two positively correlated (*Lactobacillus_plantarum* and *Alistipes_putredinis*) with the active avoidance response (Figure 4E). Of these, *L. plantarum* was positively correlated with cognitive performance in the Morris water maze and shuttle-box tests.

Medicinal foods, specifically probiotics, have recently materialized as a tool to manage various intestinal disorders. Indeed, the synthesis of microflora-dependent

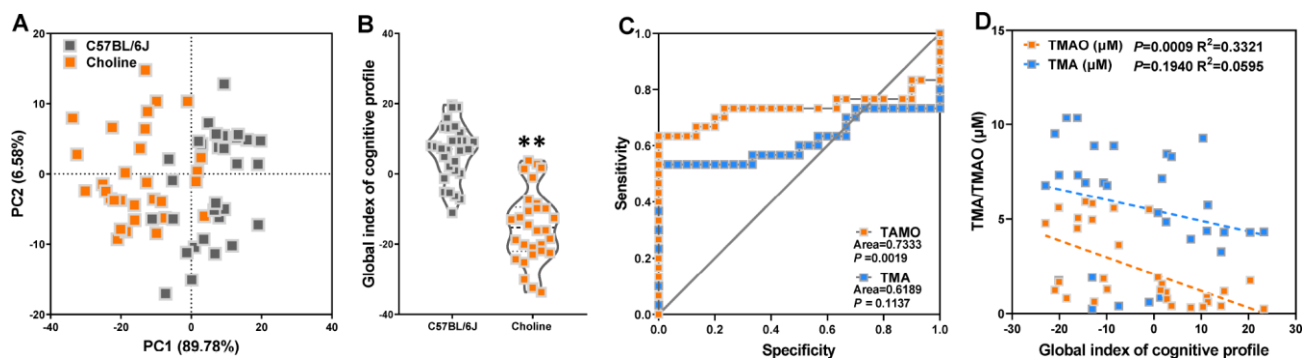


Figure 3. Increased plasma TMAO levels are associated with cognitive declines in C57BL/6J mice. Principal component analysis (PCA) data derived from behavioral experiments of mice with or without choline supplementation (A). Each axis was derived by PCA. Each point represents one of the mice with or without choline. Principal component 1 (variance explained: 89.78%), principal component 2 (variance explained: 6.58%) considered significant variance with a load below or equal to 0.50 (absolute value). The mean PCA scores of mice with or without choline (B). Receiver operating characteristic (ROC) curve plots for distinguishing choline-treated mice from control mice based on a TMA- or TMAO-based random forest model (C). Spearman correlation between the TMA, TMAO concentrations and cognitive impairments in WT and APP/PS1 mice (D). ** $P < 0.01$, versus the C57BL/6J mice, by unpaired Student's *t*-tests. All values are mean \pm S.D. $n = 30$.

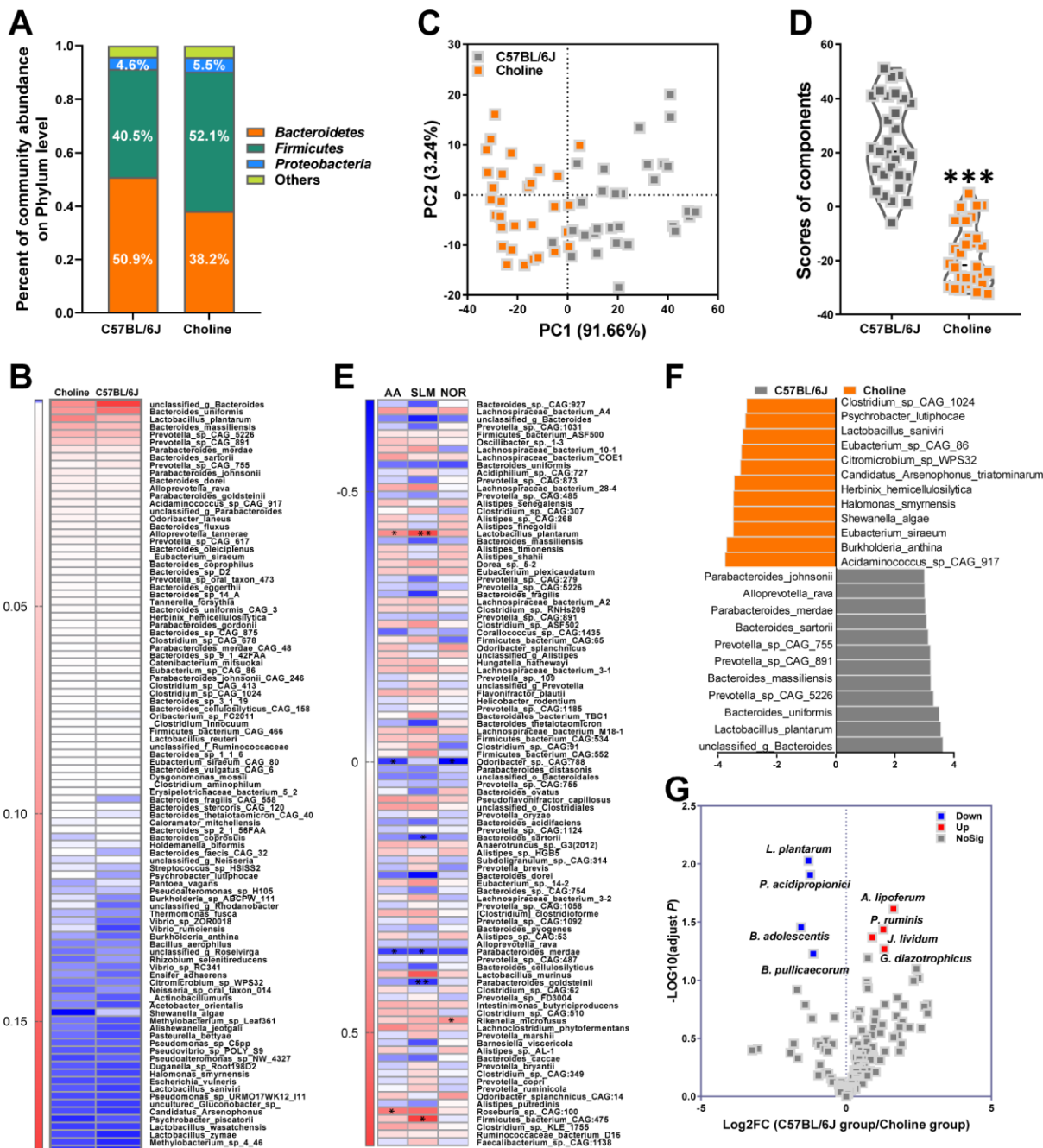


Figure 4. Effects of choline supplementation on microbial remodeling in C57BL/6J mice. Metagenomic analyses of feces at the phylum level (A). Heat map of metagenomic analyses of feces at the species level. The scale reveals the data as follows: red represents high values and blue represents low values for the percentages of reads that were classified at that rank (B). PCA at the species level in each group (C) and average PCA scores (D). *** $P < 0.001$, versus the C57BL/6J mice, by unpaired Student's t -tests. All values are mean \pm S.D. $n = 30$. Correlation heat map demonstrating the association between the indicated microbiota taxonomic species and cognitive abilities from mice grouped by dietary status (chow and choline) (E). Red denotes a positive correlation, blue denotes a negative correlation, and white denotes no correlation. A single asterisk indicates a significant FDR-adjusted correlation at $P < 0.05$, and two asterisks indicate a significant FDR-adjusted correlation at $P < 0.01$. NOR = novel object recognition memory; SLM = spatial learning and memory; AA = active avoidance. The taxa most differentially abundant between the mice with or without choline at the species level were identified by linear discriminant analysis (LDA) coupled with effect size measurements (F). Choline-diet-enriched taxa are indicated with a negative LDA score (orange), and taxa enriched in the normal chow diet have a positive score (gray). Only taxa meeting an LDA significant threshold value of >3 are displayed. Volcano plots are used to visualize the differential probiotics expression between the mice with or without choline (G). The red points in the plot represent the differentially increased probiotics, the blue points represent the differentially decreased probiotics, the gray points represent the no changed probiotics with statistical significance.

TMAO from choline-containing precursors might be reduced by some probiotics [15]. A probiotics database termed PROBIO is a knowledge-based database of probiotics functions and lineages [16]. In this study, clusters of probiotics were annotated for their characteristic sequences by best-hit against a PROBIO database and identified and grouped into 135 probiotics (Figure 4G). For choline-fed mice, the relative abundances of *Lactobacillus plantarum*, *Propionibacterium acidipropionici*, *Butyricicoccus pullicaecorum*, and *Bifidobacterium adolescentis* were lower, and the relative abundances of *Anthinobacterium lividum*, *Pseudobutyrvibrio ruminis*, *Gluconacetobacter diazotrophicus*, and *Azospirillum lipoferum* were higher than those in the control group. Notably, *L. plantarum* was associated with cognitive declines and plasma TMAO levels in choline-treated mice (Supplementary Figure 1). Thus, in subsequent experiments, we attempted to assess the effects of *L. plantarum* on cognitive impairments in an AD mouse model via modulation of TMAO generation.

Effect of *L. plantarum* supplementation on cognitive impairments in APP/PS1 mice

To determine the effect of *L. plantarum* treatment on cognitive behavior of a transgenic AD mouse model, we subjected mice to the novel object recognition test, the Morris water maze test, and the shuttle-box test. Six-month-old male WT non-transgenic littermates and APP/PS1 mice were selected, which received sterilized PBS, a dose of 1 mg/mL memantine, 1×10^9 CFU/mL *L. plantarum*, and 1 mg/mL memantine and 1×10^9 CFU/mL *L. plantarum*, respectively. Treatments were administered to the mice once a day by oral gavage. After a three-month treatment, novel object recognition testing revealed a decreased preferential index among APP/PS1 mice in short-term memory (Figure 5A). However, treatment with memantine alone or in combination with *L. plantarum* improved these animals' short-term memory. In the Morris water maze test, APP/PS1 mice had longer escape latencies compared with WT mice on the last learning day, and the latencies in the memantine-, *L. plantarum*-, or combination-treated APP/PS1 mice were shorter than those in the model group (Figure 5B). In the testing phase, the mean escape latency was longer (Figure 5C), the time in the target quadrant was shorter (Figure 5D), and the number of plate crossings diminished (Figure 5E); however, there was no difference in swimming speed (data not shown) in APP/PS1 mice compared with WT mice. Escape latencies were reduced in combination- or memantine-treated APP/PS1 mice, and the time in the target quadrant was reversed in mice treated with memantine, *L. plantarum*, or combination while the number of plate crossings expanded only in the combination-treated group. In the shuttle-box test, there was a decrease in

avoidance times in APP/PS1 compared with WT mice; however, this was rescued after the administration of combination treatments (Figure 5F). Spearman correlation analysis showed that between the circulating TMA/TMAO/FMAO3 levels and global index of cognitive profile in WT and APP/PS1 mice. TMA and TMAO levels were correlated with the global index of cognitive profile (Supplementary Figure 2). These findings showed that *L. plantarum* augmented the effects of memantine in the treatment of short-term object recognition memory, spatial learning and memory, and active avoidance response deterioration in AD mice.

Effect of *L. plantarum* supplementation on long-term potentiation (LTP) decline in APP/PS1 mice

LTP is a putative neuromechanism of associative memory formation and preservation related to cognition capacity [17]. The average population spike (PS) amplitude of APP/PS1 mice decreased after HFS (Figure 6). On the other hand, the average PS amplitude of APP/PS1 mice was elevated by the treatment with memantine, *L. plantarum*, and combination, compared to that of controls. Spearman correlation analysis showed that TMA and TMAO levels correlated with LTP (Supplementary Figure 3).

Effects of *L. plantarum* supplementation on hippocampal A β plaques in APP/PS1 mice

A β plaques in the cerebrum is the most common pathological hallmark of AD in patients and animal models. We performed immunofluorescent staining of brain slices stably expressing human A β with the antibody 6E10, which labels A β . Our results demonstrated that APP/PS1 mice developed numerous A β plaques in the brain at nine months while WT mice did not (Figure 7A). Memantine-, *L. plantarum*-, and combination-treated APP/PS1 mice showed a reduction of A β plaques in the hippocampus (Figure 7B). AlphaLISA assay showed that the concentration of A β_{1-42} and A β_{1-40} in the hippocampus of APP/PS1 mice was higher than that in WT mice (Figure 7C and 7D). Spearman correlation showed that TMA and TMAO levels correlated with A β plaques, A β_{1-42} and A β_{1-40} levels in the hippocampus (Supplementary Figure 4). These data indicated that while all treatments inhibited A β , combination treatment showed the strongest effect and Memantine alone showing the weakest.

Effects of *L. plantarum* supplementation on hippocampal neurons and plasticity in APP/PS1 mice

To determine the effects of *L. plantarum* on hippocampal neurons and plasticity, we measured the

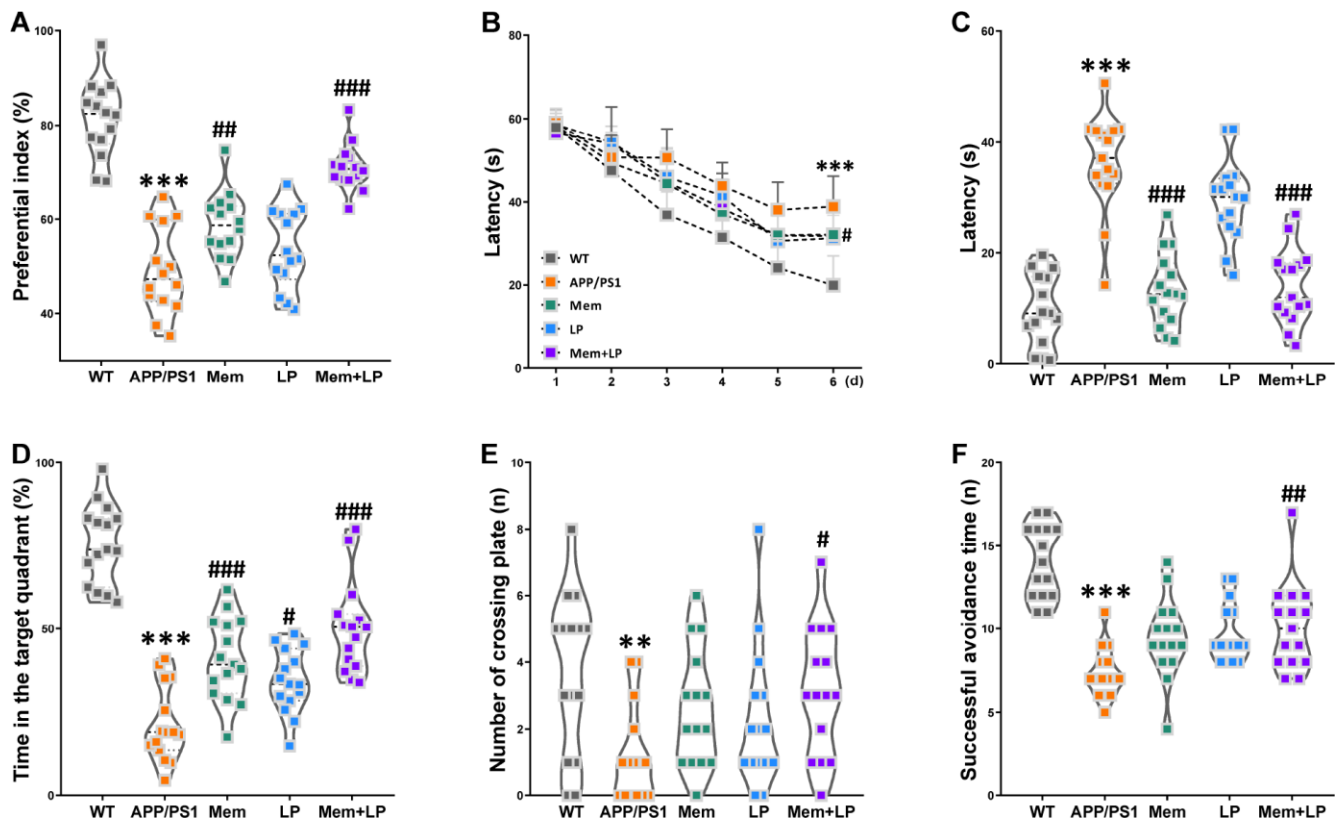


Figure 5. Effect of *L. plantarum* supplementation on cognitive impairments in APP/PS1 mice. APP/PS1 mice were treated with memantine, *L. plantarum*, or memantine+*L. plantarum*. The preferential index after training 1 hour (A) in the phase of novel object test, latency in the learning phase (B), latency (C), time spent in target quadrant (D) and number of crossing plate (E) in the testing phase of Morris water maze test, successful avoidance times in testing phase (F) of shuttle box test. ** $P < 0.01$, *** $P < 0.001$, versus the WT mice, by unpaired Student's *t*-tests. # $P < 0.05$, ## $P < 0.01$, ### $P < 0.001$, versus the APP/PS1 mice, by one-way ANOVA analysis followed by Dunnett's *post hoc* test or a two-way repeated-measures ANOVA with *post-hoc* Tukey multiple comparisons test. All values are mean \pm S.D. $n = 15$. WT=wild type; Mem=memantine; LP=*L. plantarum*.

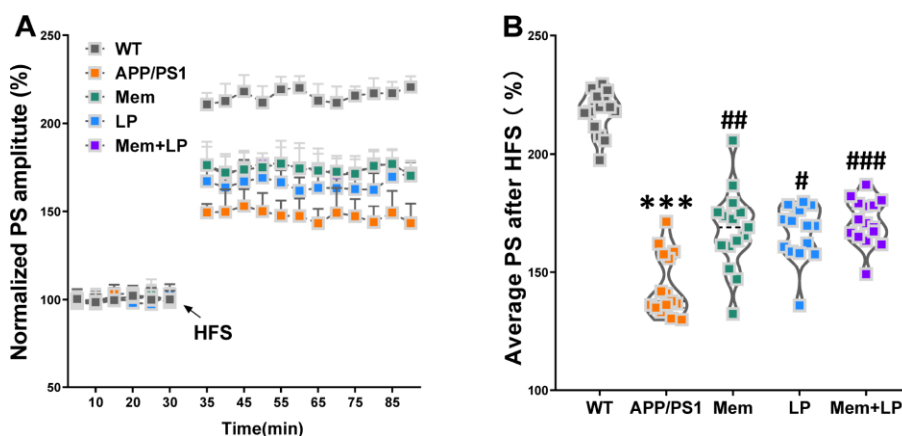


Figure 6. Effect of *L. plantarum* supplementation on long-term potentiation (LTP) decline in APP/PS1 mice. The population spike (PS) amplitudes and LTP induction were recorded in WT and APP/PS1 mice (A). Summary of average PS amplitude (31-90 minutes) from all experiments shown in A (B). *** $P < 0.001$, versus the WT mice, by unpaired Student's *t*-tests. # $P < 0.05$, ## $P < 0.01$, ### $P < 0.001$, versus the APP/PS1 mice, by one-way ANOVA analysis followed by Dunnett's *post hoc* test. All values are mean \pm S.D. $n = 15$. W=wild type; Mem=memantine; LP=*L. plantarum*.

amount of Nissl bodies and dendritic spine density using Nissl and Golgi staining. Nissl staining showed neuropathological alterations in the hippocampus of APP/PS1 mice compared to WT mice (Figure 8A), such as fewer Nissl bodies (Figure 8B), which was partially rescued by combination treatment. Golgi staining demonstrated that APP/PS1 mice had decreased dendritic spine density in the hippocampus, which was attenuated by combination treatment (Figure 8C). We also investigated the levels of synaptic proteins, including synaptophysin and PSD95 (Figure 8D and 8E). Spearman correlation showed that TMA and TMAO levels correlated with hippocampal neuron integrity and plasticity (Supplementary Figure 5). We found that APP/PS1 mice had decreased levels of synaptophysin and PSD95, which were improved by memantine and combination treatments. On the other hand, *L. plantarum* administration elicited only a modest increase in PSD95 expression. These data revealed that addition of *L. plantarum* to the treatment of APP/PS1 mice treated with memantine protected hippocampal neurons and plasticity.

Effects of *L. plantarum* supplementation on TMAO synthesis in APP/PS1 mice

Alterations in the composition of gut flora can reduce intestinal TMA levels, leading to decreased TMAO synthesis in the liver. As shown in Figure 9, treatment with *L. plantarum* or a combination of memantine and *L. plantarum* markedly decreased TMA and TMAO levels and increased hepatic FMO activity while FMO3 levels in the liver remained unchanged. These results were consistent with our observation in C57BL/6J mice, suggesting an important role for the intestinal microbiome in reducing TMAO levels.

Effects of *L. plantarum* supplementation on the levels of clusterin in plasma and inflammatory status in the hippocampus of WT and APP/PS1 mice

Increased clusterin levels in plasma promoted the accumulation of fibrillar A β aggregates in AD mouse brains while clopidogrel inhibited it [18]. In our study, APP/PS1 mice had a higher concentration of clusterin in

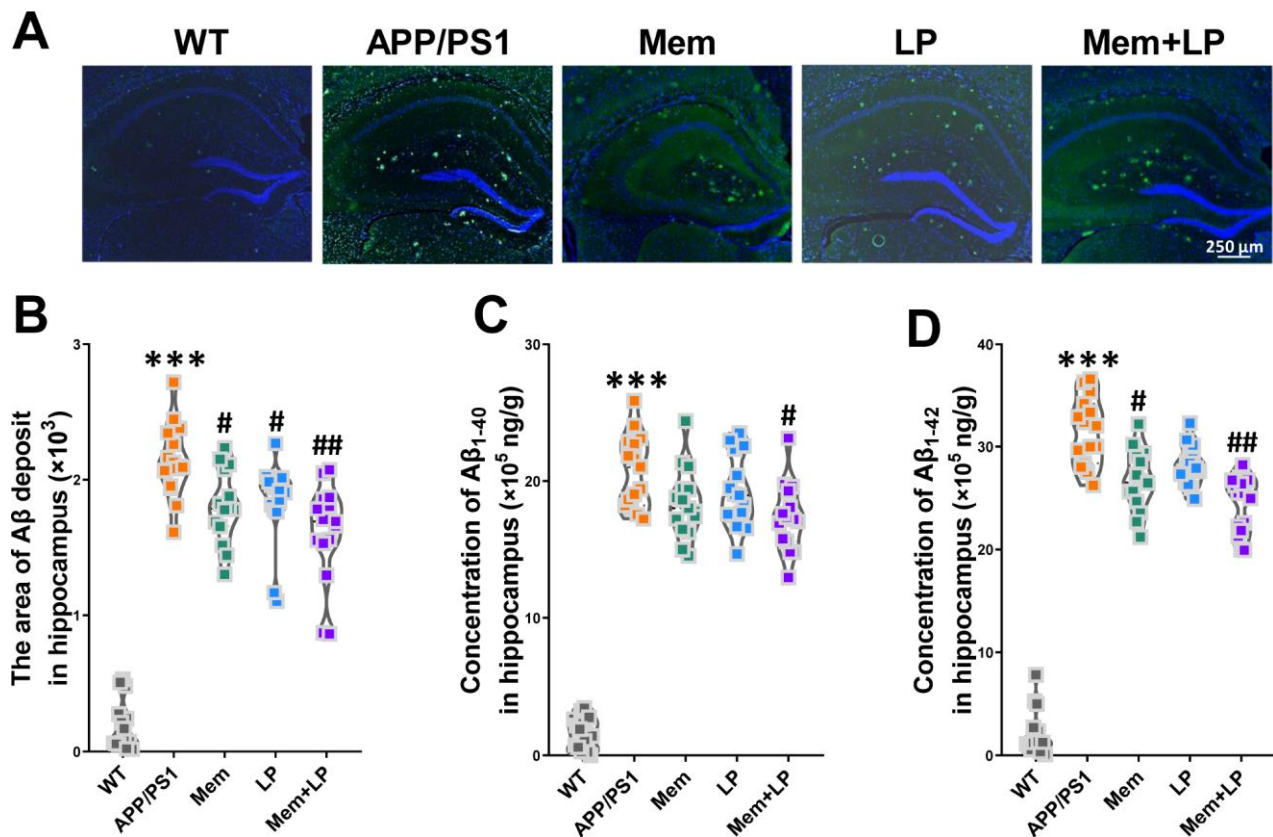


Figure 7. Effect of *L. plantarum* supplementation on A β deposition in APP/PS1 mice. Representative immunofluorescence staining images showing A β plaques (green and indicated by red arrows) in the hippocampus of WT and APP/PS1 mice (A). Quantitative analysis of A β plaques (B), A β ₁₋₄₀ (C) and A β ₁₋₄₂ (D) in the hippocampus was used by Image Pro Plus 6.0 software and AlphaLISA assay. ****P*<0.001, versus the WT mice, by unpaired Student's *t*-tests. #*P*<0.05, ##*P*<0.01, versus the APP/PS1 mice, by one-way ANOVA analysis followed by Dunnett's post hoc test. All values are mean ± S.D. n=15. WT=wild type; Mem=memantine; LP=*L. plantarum*.

plasma than WT mice (Figure 10A), which was reduced by treatment with *L. plantarum* or the combination of memantine and *L. plantarum*. Given established correlations between clusterin levels in plasma and numerous immunomodulatory regulators, clusterin might constitute a potential therapeutic target to treat irregular immune responses in the AD cerebrum [19]. Therefore, we used multiplex bead analysis to comprehensively measure inflammation in the hippocampus (Figure 10B). We found a significant increase in hippocampus levels of

proinflammatory cytokines, including the classical mediators IL-1 β , IL-2, IL-6, IL-17, IFN γ , TNF- α , RANTES, and Eotaxin in APP/PS1 mice. On the other hand, neuroinflammation in the hippocampus was reduced in *L. plantarum*- or combination-treated mice, as shown by the reduction in IL-2 (Figure 10C), IL-17 (Figure 10D), and TNF- α (Figure 10F) concentrations. Thus, suggests that *L. plantarum* attenuated neuroinflammation by reducing clusterin levels via inhibition of TMA production and TMAO synthesis.

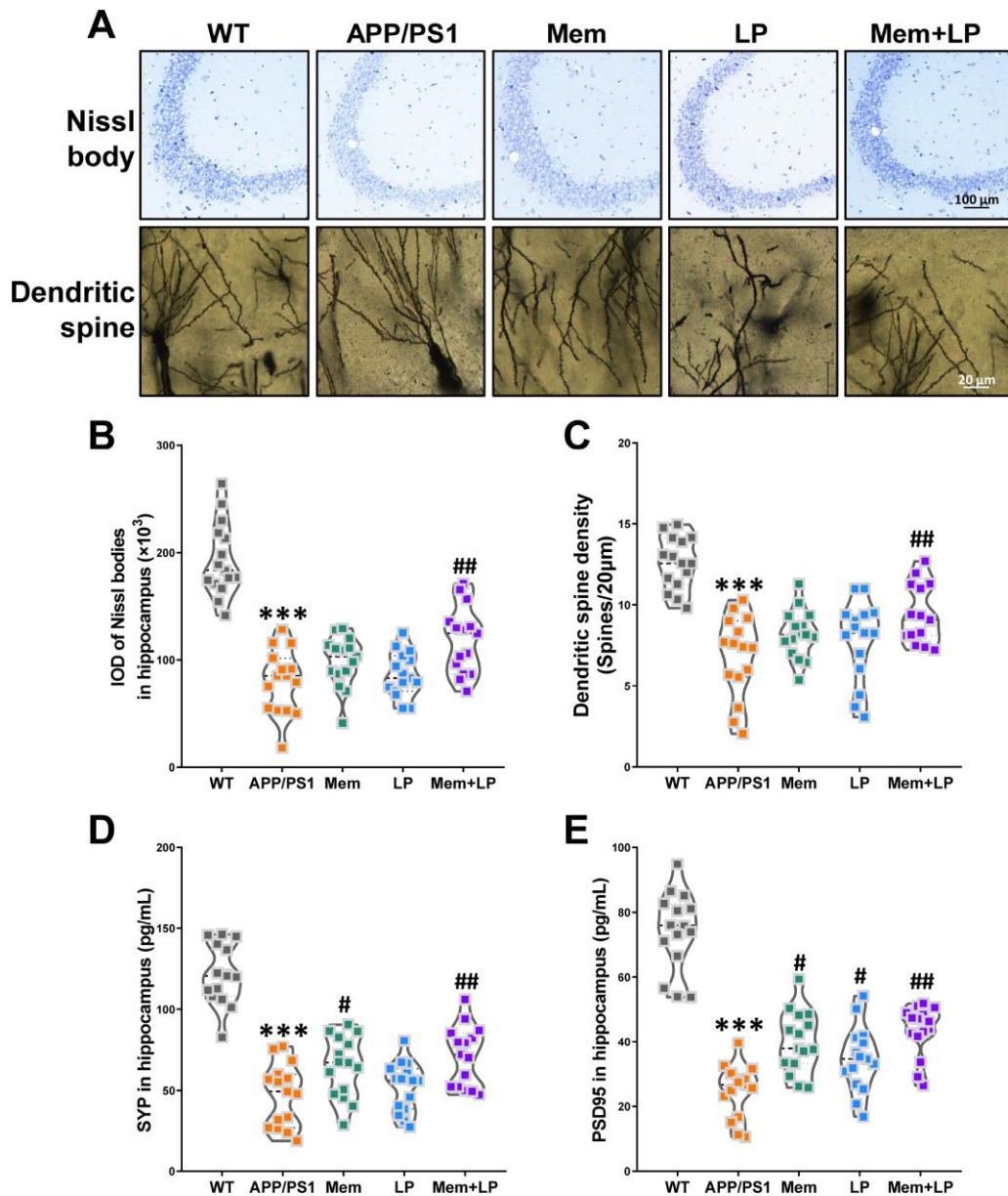


Figure 8. Effects of *L. plantarum* supplementation on hippocampal neuron and plasticity in APP/PS1 mice. Representative images of Nissl staining images (upper panel) and dendritic spines (lower panel) under microscopy in the hippocampus of WT and APP/PS1 mice (A). Quantification of and Nissl bodies (B) and mean dendritic spine density (C). The expression of hippocampal synaptophysin (D) and PSD95 protein (E). *** $P < 0.001$, versus the WT mice, by unpaired Student's *t*-tests. # $P < 0.05$, ## $P < 0.01$, versus the APP/PS1 mice, by one-way ANOVA analysis followed by Dunnett's *post hoc* test. All values are mean \pm S.D. $n = 15$. WT=wild type; Mem=memantine; LP=*L. plantarum*.

DISCUSSION

In the current study, we found that *L. plantarum* decreased TMAO levels by suppressing gut microbial TMA secretion via remodeling of gut microbiota in transgenic AD mice, thereby attenuating cognitive impairments and pathological deterioration. To the best of our knowledge, this is the first study demonstrating the role of TMAO in *L. plantarum*-induced protection against AD. Moreover, the addition of *L. plantarum* to memantine treatment potentiated the therapeutic benefits of memantine alone by decreasing the concentration of A β ₁₋₄₂ and A β ₁₋₄₀, protecting hippocampal neurons and plasticity, inhibiting TMAO synthesis, and alleviating neuroinflammation.

Dietary choline is metabolized by the gut microbiota into TMA, which is converted by FMO3 into hepatic TMAO. The intestinal metabolite TMAO contributes to the pathogenesis of AD [20]. Indeed, CFS TMAO levels are higher in AD patients than in cognitively-unaffected individuals [6] and correlated with AD susceptibility and pathogenicity [5]. Furthermore, elevated circulating TMAO reduced hippocampal antioxidant enzyme levels [21], induced cognitive dysfunction, and accelerated brain aging [22]. Here, feeding C57BL/6J mice diets enriched in choline resulted in declines in novel object recognition memory, spatial learning and memory, and active avoidance response. In addition, dietary choline supplementation elevated TMA and TMAO levels in plasma but cognitive decline correlated only with the latter.

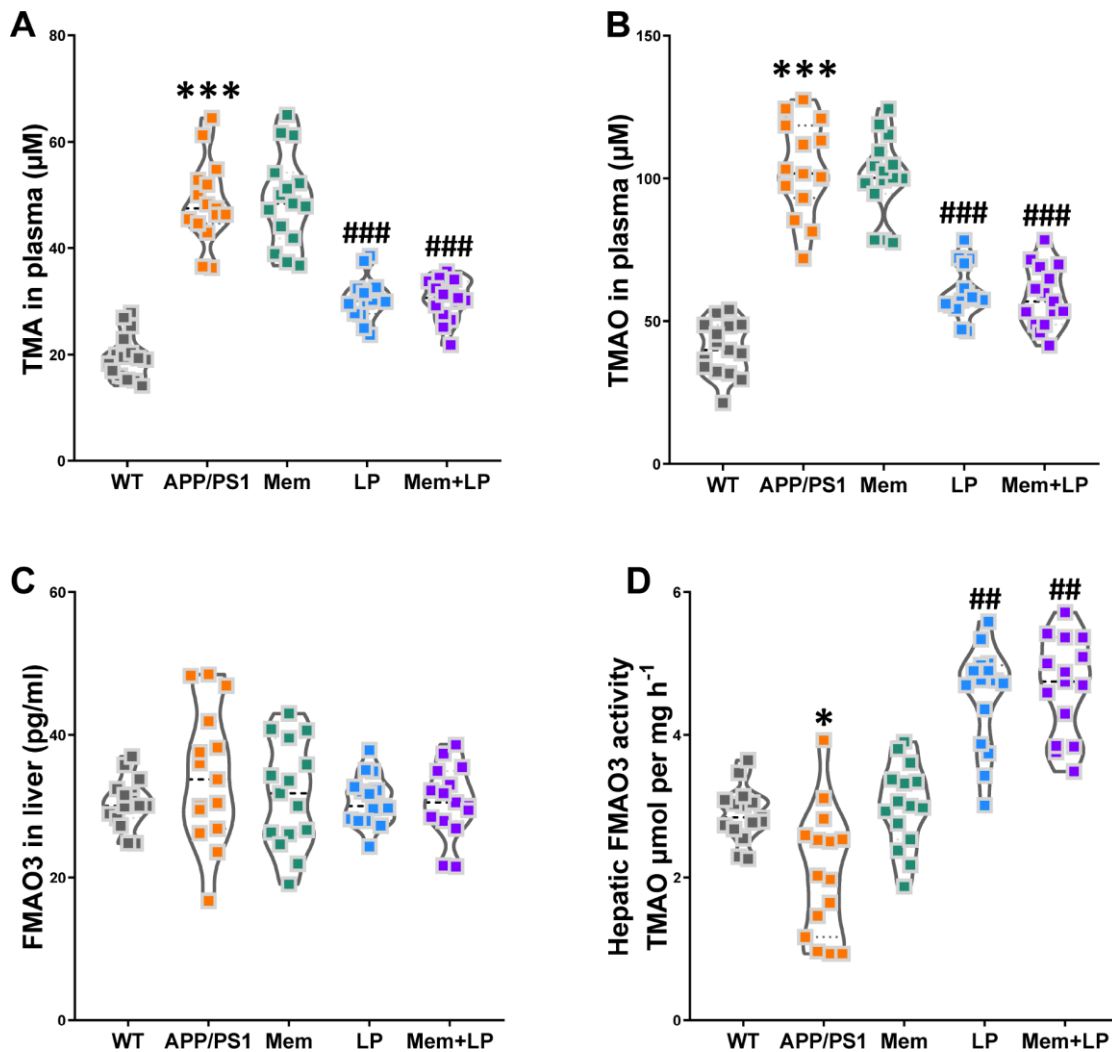


Figure 9. Effects of *L. plantarum* supplementation on TMAO synthesis in APP/PS1 mice. The concentration of TMA (A), TMAO (B) in plasma, and FMO3 (C) in the liver. Liver FMO activity, assessed as described in Materials and Methods (D). *** $P < 0.001$, versus the WT mice, by unpaired Student's *t*-tests. # $P < 0.05$, ## $P < 0.01$, ### $P < 0.001$, versus the APP/PS1 mice, by one-way ANOVA analysis followed by Dunnett's *post hoc* test. All values are mean \pm S.D. $n = 15$. WT=wild type; Mem=memantine; LP=*L. plantarum*.

The gut microbiota and its host are symbiotically related. The intestine has been defined as the second brain, because it can affect psychological, emotional, and cognitive homeostasis [23–25], evidencing the functional influence the gut and the cerebrum can have on each other. Alterations in the relative abundance of intestinal flora correlated with increased concentrations of phosphorylated *tau* and with an increased $A\beta_{1-40}/A\beta_{1-42}$ ratio in AD patients [26]. Similarly, intestinal mucosal barrier dysfunction correlated with increased fecal calprotectin concentrations [27], and a specific gut microbiome composition correlated to AD histological and behavioral hallmarks in APP/PS1 mice [28]. Moreover, colonization of germ-free APP transgenic mice with intestinal flora from conventionally-raised APP transgenic mice increased cerebral $A\beta$ pathology, and vice versa [29]. Hence, gut microbiota alternations might accelerate the appearance of AD-like cognition decline and lesions. Our study showed that there were that gut microbiota were differentially abundant in control mice and choline-treated mice. Furthermore, we found that abundance of *L. plantarum* correlated with

cognitive declines and plasma TMAO levels in choline-administrated mice based on data from the PROBIO database.

Probiotics are regarded as a novel and harmless way of stabilizing a healthy gut microbiota by competing with other intestinal bacteria for binding sites or receptors on the mucosa [30], or by secreting metabolic compounds that restrain the growth of other microorganisms [31, 32]. Probiotic administration can also induce neuronal plasticity and elicit improvements in behaviors associated with psychiatric conditions. For instance, probiotics appear to protect neurogenesis in the brain as measured by increases in brain-derived neurotrophic factors, which in turn can reduce inflammatory cytokines and oxidative stress [33]. In addition to improving the immune functions of the host, probiotics can balance gut microbiota to produce states that are advantageous to beneficial microorganisms [34], as seen in clinical studies. Indeed, probiotic supplementation improved cognitive and emotional symptoms in AD patients as well as metabolic function, supporting the

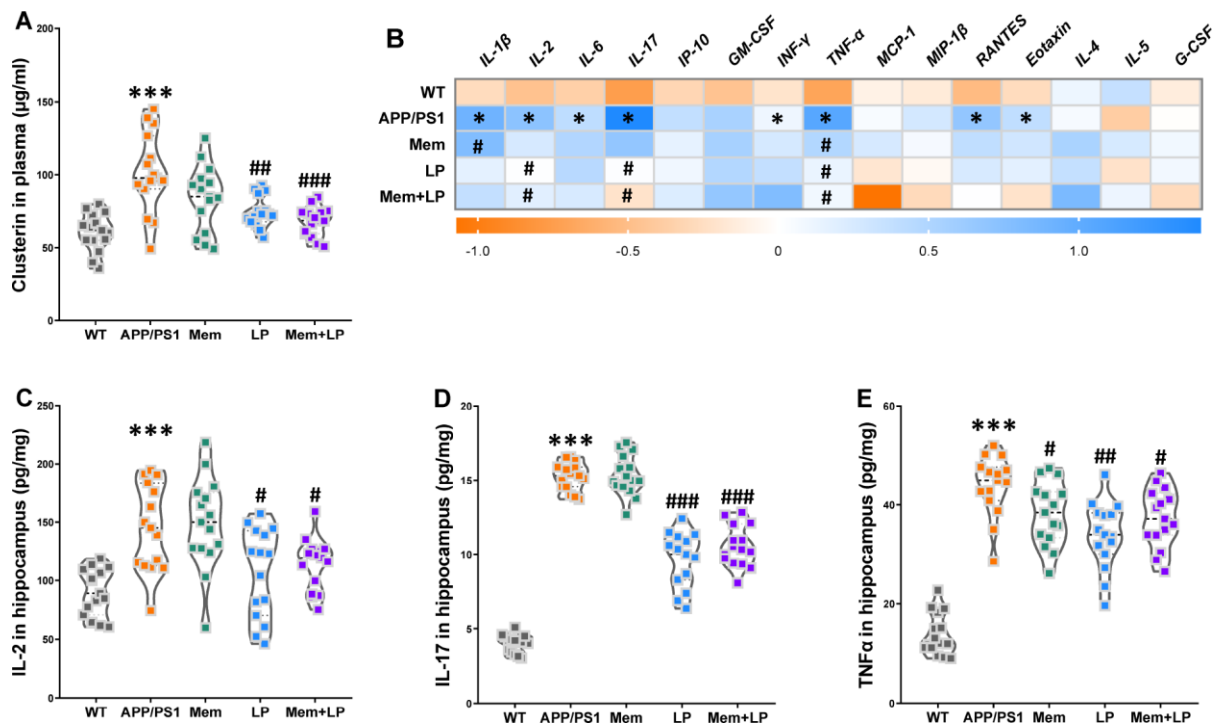


Figure 10. Effects of *L. plantarum* supplementation on the levels of clusterin in plasma and inflammatory status in the hippocampus of WT and APP/PS1 mice. The concentration of plasma clusterin (A). Heat map of cytokine concentrations (z-score) in the hippocampus (B). * represents a difference between WT and APP/PS1 mice, # represents a difference between APP/PS1 mice and treated APP/PS. The concentration of interleukin (IL)-2 (C), IL-17 (D) and tumor necrosis factor α (TNF α) (E) in the hippocampus. *** $P < 0.001$, versus the WT mice, by unpaired Student's *t*-tests. # $P < 0.05$, ## $P < 0.01$, ### $P < 0.001$, versus the APP/PS1 mice, by one-way ANOVA analysis followed by Dunnett's *post hoc* test. All values are mean \pm S.D. $n = 15$. WT=wild type; Mem=mementine; LP=*L. plantarum*. IL=interleukin; IP=interferon-induced protein; GM-CSF=granulocyte-macrophage colony-stimulating factor; INF γ =interferon- γ ; TNF- α =tumor necrosis factor α ; MCP-1=monocyte chemotactic protein-1; RANTES=regulated upon activation normal T cell expressed and secreted factor; MIP-1 β =macrophage inflammatory protein-1 β ; G-CSF=granulocyte colony-stimulating factor.

hypothesis that probiotics can activate specific brain regions involved in the control of emotion and sensation [35]. Some studies have shown that western diets can promote anxiety but supplementation with *L. helveticus* can prevent this effect [36]. Similarly, supplementation with various probiotic strains has been observed to improve cognitive functions and alleviate symptoms in several diseases such as diabetes [37], among others [38]. VSL#3, a probiotic mixture containing eight Gram-positive probiotic strains, modulated the expression of genes that impact inflammatory and neuronal plasticity processes in brain tissue, attenuated age-related deficits in LTP, and decreased microglial activation markers while increasing synapsin expression [39]. Here, we observed that *L. plantarum* augmented the effects of memantine in the treatment of cognitive deterioration in APP/PS1 mice. Moreover, combination treatment with memantine and *L. plantarum* attenuated hippocampal LTP deficits, decreased intracerebral A β deposits and the abundance of other species including oligomers, and reduced A β_{1-42} and A β_{1-40} levels while protecting neuronal integrity and plasticity in the hippocampus. Therefore, our findings suggest that *L. plantarum* might augment the therapeutic effects of memantine on AD-like cognition and neuropathology impairments in APP/PS1 mice.

Emerging evidence has revealed that gut microbiota, through the production of TMAO, directly contribute to platelet hyperreactivity [7]. Moreover, circulating TMAO was not strictly correlated with differences between vegetarian and omnivorous diets [8, 40]. Yet, TMAO levels might be affected by modifications in gut microbiota composition, which possibly modulate TMA production [41]. TMAO increases the risk of thrombosis [7], disruption of hormonal homeostasis [42], and inflammation [43]. Here, we found that *L. plantarum* and the combination of memantine and *L. plantarum* inhibited TMAO synthesis by decreasing gut microbial TMA production through gut microbiota modulation, which subsequently attenuated cognition and neuropathology deficits in APP/PS1 mice. Meanwhile, a recent report revealed that 3,3-dimethyl-1-butanol could reduce TMAO levels by inhibiting the formation of TMA from microbes in aged rodents, thereby attenuating inflammation and oxidative stress [44]. These results suggested that targeting the intestine microbial generation of TMA distinctively through probiotic supplementation may serve as an effective therapeutic strategy for AD.

Clusterin is a versatile glycoprotein that promotes AD progression and modifies the structure of A β [45], consistent with results from clinical trials [46, 47]. The effects of clusterin on A β accumulation and might depend on the ratio between their levels [48, 49].

Similarly, fibrillar A β deposits in PDAPP mice expressing clusterin were more abundant than clusterin-knockout PDAPP mice, even though the general abundance of deposits was comparable, suggesting that clustering might stabilize a specific subset of A β conformations [50]. Clusterin knockout in APP/PS1 mice demonstrated a noticeable decrease in cerebral A β deposits and decreased inflammation [51]. Regarding immune mechanisms, complement components were identified as particular risk factors for AD by GWAS [52, 53], with clusterin modulating the complement system and various cytokines, including TNF- α [54], IL-2 [55], IL-17 [56], and membrane attack complex [57]. In our study here, we found high levels of clusterin and proinflammatory cytokines in the hippocampus of APP/PS1 mice and observed that treatment with *L. plantarum* or a combination of memantine and *L. plantarum* reduced such levels.

A limitation of our study is that we do not address the molecular mechanisms underlying the therapeutic effects we have uncovered *L. plantarum* and combination treatments. We speculate that TMAO might indirectly alter signaling pathways by altering the conformation of its protein partners. Indeed, TMAO can directly stabilize protein folding and induce conformational changes in proteins by functioning as a small-molecule protein chaperone [58, 59]. It is thus conceivable that TMAO might modify numerous signaling pathways without directly activating a specific TMAO receptor. Nonetheless, our results here showing that *L. plantarum* augments the beneficial effects of memantine on AD open a new avenue of research and highlight the intestinal microbiota as an exciting target for pharmacological or dietary interventions to decrease the risk of AD.

MATERIALS AND METHODS

Animals and treatments

Eight-week-old male C57BL/6J mice ($n=60$) were obtained from Jackson Laboratory (Bar Harbor, USA). For all the experiments, mice were kept and fed individually and had random access to potable water. Mice in the control group ($n=30$) were fed a standard chow diet, and the model group ($n=30$) was fed a chow diet supplemented with 1% choline for three months. Mice were weighed every week and were maintained at the animal experimental center of Harbin medical university in a temperature-controlled environment ($22 \pm 2^\circ\text{C}$), with a 12-h light/dark cycle. Animal experiments were carried out in accordance with the references in the Guide for the Care and Use of Laboratory Animals published by the National Institutes of Health and were approved by the Institutional

Animal Care and Use Committee of Harbin medical university.

Six-month-old male wild type (WT) non-transgenic littermates and PrP-hA β PP^{swe}/PS1^{ΔE9} transgenic (APP/PS1) mice with a C57BL/6 genetic background were obtained from Jackson Laboratory (Bar Harbor, USA). *Lactobacillus plantarum* ATCC 8014 was purchased from ATCC, via the Beijing BioChen Co. Ltd. *L. plantarum* was stored in 15% glycerol at -80 °C and anaerobically cultured in DeMan-Rogosa-Sharpe (MRS) agar at -37 °C. *L. plantarum* cell pellets were collected and washed with PBS (8000 rpm for 15 min). The harvested pellet was resuspended in PBS comprising 15% glycerol to prepare the concentration of 5×10⁹ CFU/mL and subsequently stored at -80 °C until use for oral administration to mice. After a three-day adaptation period, the mice were randomly separated into seven groups (*n*=15 mice per group) as follows: control group (WT mice) and model group (APP/PS1 mice), which received sterilized PBS (pH 7.4); memantine group (APP/PS1 mice), which received a daily dose of 1 mg/mL memantine (Sigma-Aldrich, USA); *L. plantarum* group (APP/PS1 mice), which received a daily dose of 1×10⁹ CFU/mL *L. plantarum*; combination group (APP/PS1 mice), which received a daily dose of 1 mg/mL memantine and 1×10⁹ CFU/mL *L. plantarum*. Treatments were administered once a day for 12 weeks by oral gavage. Following behavioral tests and electrophysiological measurements, mice were placed in a sealed chamber and euthanized via isoflurane inhalation and cervical dislocation. The hemisphere and plasma of each mouse were collected for biochemical and histochemical analyses.

Behavioral experiments

Spontaneous locomotor activity test

The spontaneous locomotor activity proceeded for 20 min. Spontaneous locomotor behavior was recorded by a video-based behavior monitoring system (XinRan Technology, China).

Nest building test

Mice were placed into individual testing chambers with one nestled (4 cm squares). The nesting score was calculated at the following morning by a pre-determined measuring scale (least: 1, best: 6).

Novel object recognition test

The testing paradigm of the object recognition test consisted of three phases: familiarization, training, and testing. Generally, to be familiar with the testing condition, mice freely explored an empty chamber (10 min daily) for two days. On the third day, mice explore two similar objects (object A1 and A2) that are

averagely placed at opposing ends of the chamber. Object exploration was described as the time mice spent bodily contacting the object within 0.2 cm. Each mouse explored similar objects for 10 min. After a 1-hour and 24-hour training-to-testing interval, a novel object (object B or C) was taken the place of one of the same objects. The preferential index (time on object B or C/(time on object B or C+time on object A)×100%) was calculated to evaluate object recognition memory in 5 min phase.

Morris-water maze test

Morris-water maze test was conducted in a white circular pool (diameter: 90 cm and depth: 45 cm). The pool was filled with 30-cm-depth water. The water temperature was kept at 20 ± 1°C by adding ice water. The platform of diameter 6 cm was placed 1 cm underneath the water. The training and testing periods were 60 s. In the training period, mice finished four trials daily for five consecutive days with a hidden platform. Mice that did not discover the platform within 60 s were guided towards the hidden platform and put onto the platform for 5 s. In the testing period, the platform was removed and the mice were allowed to search for the disappeared platform for 60 s. The latency to find the hidden platform in the training and testing periods and the time spent in the target quadrant was recorded and analyzed.

Shuttle-box test

In the shuttle box test, all avoidance training phases consisted of 30 trials with the following parameters: 15 s tone (50 dB) and light (9W), 5 s foot shock (0.25 mA), and 15 s training-to-testing interval. A testing phase with the same parameters without foot-shock, after the 7 consecutive days, was carried out. The argument automatically recorded was the successful active avoidance times.

Electrophysiology

The mice were anesthetized by 1.0 g/kg urethane intraperitoneal injection and positioned in a stereotaxic frame (Narishige). A bipolar stimulating electrode was inserted in the perforant path (anterior to lambda: 0.6 mm, to midline: 2.4 mm, to brain surface: 1.7-2.1 mm). The evoked potentials were received with an electrode at the dentate gyrus (-2.0 mm, 1.0 mm, 1.7-2.2 mm). The electrical stimulus produced by the stimulator. The pulses (0.1 ms, 1/60 Hz) transmitted through an isolator (Nihon Kohden) to provide a steady electric current. The evoked responses were amplified and low-pass filtered (1000 Hz, Axon Instruments), then transmitted through a data acquisition system (Digidata 1200, Axon Instruments). After obtaining a steady stimulus-response curve, a 1/2 maximum population spike (PS) was applied. Following a recording (30 min), the long-

term potentiation (LTP) was induced by high-frequency stimulation (HFS), and the PSs of each mouse were recorded (31-90 minutes).

Histochemical and biochemical analyses

Immunofluorescence

Hemispheres were collected and fixed in 4% paraformaldehyde, then embedded by paraffin. The 5- μ m-thick tissue sections were prepared. Subsequently, sections were incubated overnight at 4 °C with primary antibodies for β -amyloid (6E10, Biolegend, USA). After being washed three times in PBS, the sections were incubated with goat anti-mouse IgG HRP (1:1000, ZSGB-Bio, Beijing, China) for 2 h at room temperature, then incubated with Opal™ 6-Color Fluorescent IHC Kit (PerkinElmer, USA) for 15 min, and mounted with DAPI-containing medium. Sections were digitized by a fluorescence imaging microscopy (Vectra 2, PE-Caliper LS, USA). The area of A β plaque was calculated by Image Pro Plus 6.0 software.

Nissl staining

The sections were stained by 0.5% cresyl violet acetate (Beyotime, China) and photographed using a transmission electron microscope (TEM)(Hitachi, Japan). The integrated optical density (IOD) of Nissl bodies in the hippocampus was calculated using Image Pro Plus 6.0 software.

Golgi staining

To investigate dendritic spine density, the cerebrums were transferred to the Golgi staining solution. Golgi staining was performed in accordance with the instructions for the FD Rapid Golgostain™ Kits (FD NeuroTechnologies, USA) on unperfused cerebrum tissue.

Soluble A β analysis

The A β AlphaLISA assay was performed in this study. The concentration of A β ₁₋₄₀ and A β ₁₋₄₂ in the hippocampus were quantified using the A β ₁₋₄₀ (AL275C, PerkinElmer, USA) and A β ₁₋₄₂ (AL276C, PerkinElmer, USA) kits according to the manufacturer instructions.

Enzyme-linked immunosorbent assay

The concentration of FMO3 in the liver was assessed using a mouse flavin containing monooxygenase 3 ELISA kit (MBS9327471, MyBioSource, USA). The levels of clusterin in plasma were assessed with a mouse clusterin quantikine ELISA kit (MCLU00, R&D Systems, USA). The levels of synaptophysin and PSD95 protein in the hippocampus were assessed using an ELISA kit for synaptophysin (CEA425Mu-1, Lifeome BioLabs, USA) and DLG4 / PSD95 ELISA Kit (LS-F7142-1, LifeSpan BioSciences, USA) according to the manufacturer's instructions. Absorbance was

measured at 450 nm with a reference wavelength of 450 nm via an Enspire™ multilabel reader 2300 (PerkinElmer, Finland).

Quantitation of TMAO and TMA levels

We added 80 μ L of 80% acetonitrile to 20 μ L of plasma for protein precipitation. As interior standards, d₉-(trimethyl) TMAO and d₉-(trimethyl) TMA were added to plasma samples. After 30 min, samples were centrifuged (20,000 \times g, 4°C, 10 min) and then analyzed by stable isotope dilution liquid chromatography-tandem mass spectrometry (LC/MS), as described previously [60]. Briefly, LC/MS analysis was performed using an Agilent 6410 Triple Quad LC/MS (Agilent Technologies, USA). The capillary voltage was heated to 350 °C and set up at +4000 V. TMAO and TMA were examined using electrospray ionization in positive-ion mode with multiple reaction monitoring and characteristic production ion transitions: *m/z* 76-58, and *m/z* 60-44. TMAO and TMA levels in plasma were quantified using an Agilent 1260 Infinity HPLC system. Chromatographic separation was carried out on a hydrophilic interaction liquid chromatography (HILIC) column (150 \times 2.1 mm, 3.5 μ m internal diameter, WATERS) shielded by a flex capillary HILIC guard column (10 \times 2.1 mm, 3.5 μ m internal diameter, WATERS). The mobile phase (phase A: methanol with 0.1% formic acid, phase B: water with 0.1% formic acid) was used at a ratio of 30:70 with a flow rate of 0.20 ml/min. The calibration curves were generated by adding various concentrations of TMAO and TMA standards to control plasma, which allowed us to quantify plasma TMAO and TMA concentrations.

Determination of the enzymatic activity of hepatic FMO

The activity of the FMO enzyme in the liver was measured as described [60], with minor alterations. Concisely, 100 mM nicotinamide adenine dinucleotide phosphate (NADPH), 100 μ M TMA, and 1 mg hepatic protein homogenate were blended in 250 μ l reaction in 10 mM HEPES buffer (pH 7.4). The reaction was terminated by adding 0.2 N formic acid after eight hours, subsequently filtering using a 3K spin filter. The mixture was then instantly stored at -80 °C. For assays, the inner standard with the thawed filtrate was injected into LC/MS to quantify the oxidized product TMAO, as mentioned above.

Multiplex bead analysis

The hippocampal supernatants were diluted at a 1:2 ratio in assay buffer and analyzed using a Luminex 200 (Luminex, USA). The cytokine expressions of interleukin-1 β (IL-1 β), IL-2, IL-4, IL-5, IL-6, IL-17, granulocyte colony-stimulating factor (G-CSF), interferon-induced protein 10 (IP-10), tumor necrosis

factor α (TNF- α), interferon- γ (IFN γ), granulocyte-macrophage colony-stimulating factor (GM-CSF), regulated upon activation normal T cell expressed and secreted factor (RANTES), macrophage inflammatory protein-1 β (MIP-1 β), monocyte chemotactic protein-1 (MCP-1), Eotaxin were measured using a multiplex map kit (MCYTOMAG-70K, Millipore, USA).

Metagenomic analyses

All feces were freely excreted by mice and then immediately collected. A total of 200-240 mg of fresh feces were collected. Total genomic DNA was extracted using an EZNA DNA kit (Omega Bio-Tek, Norcross, USA), and the purity and concentration of the extracted DNA were respectively measured using a NanoDrop 2000 spectrophotometer (Thermo Scientific, USA) and TBS-380 mini-fluorometer (Turner Biosystems, USA). The paired-end library was constructed by using a TruSeqTM DNA Sample Prep kit (Illumina Inc., USA). Paired-end sequencing was performed on the Illumina HiSeq4000 platform (Illumina Inc., USA), utilizing HiSeq 3000/4000 PE Cluster and HiSeq 3000/4000 SBS kits, according to manufacturer instructions. Adapter sequences were stripped from the 3' and 5' ends of paired-end Illumina reads by SeqPrep. Low-quality reads were removed using Sickle. Metagenomics data were assembled by MEGAHIT [61]. Contigs with a length of over 300 bp were selected for final assembly and used for further gene prediction and annotation. Open reading frames (ORFs) from each assembled contig were predicted by MetaGene [62]. All predicted genes with a 95% sequence identity were clustered using CD-HIT [63] and then mapped to representative sequences with 95% identity using a short oligonucleotide analysis package [64]. Characteristic sequences of non-redundant gene catalogs were aligned to the NCBI NR database with an e-value cutoff of $1e^{-5}$ by the basic local alignment search tool (BLAST) [65] for taxonomic annotations. Clusters of probiotics were annotated for their representative sequences employing best-hit against a PROBIO database (<http://bidd2.nus.edu.sg/probio/homepage.htm>) and with an e-value cutoff of $1e^{-5}$.

Statistical analyses

All data were expressed as mean \pm S.D. GraphPad Prism 8.0 was utilized to plot and analyze part data. Data from the two groups were compared by Student's *t*-tests. Comparison of data between multiple groups was performed using a one-way analysis of variance (ANOVA) followed by Dunnett's *post hoc* test or a two-way repeated-measures ANOVA with *post-hoc* Tukey multiple comparisons test. Spearman correlation coefficients (R, v3.1.2) were used to measure correlations between TMAO levels in plasma and

cognitive performance/pathology index. Receiver operating characteristic (ROC) curves were plotted and area under the curve (AUC) values were computed using the ROCR package in R. Principal component analysis plots were also computed using R. Results were considered statistically significant when $P < 0.05$.

Ethical approval

Animal experiments were processed in accordance with the references in the Guide for the Care and Use of Laboratory Animals published by the National Institutes of Health and were approved by the Institutional Animal Care and Use Committee of Harbin medical university.

Abbreviations

AD: Alzheimer's disease; ANOVA: One-way analysis of variance; APP: Amyloid precursor protein; AUC: Area under the curve; A β : Amyloid- β ; *L. plantarum*: *Lactobacillus plantarum*; FMOs: Flavin monooxygenases; G-CSF: Granulocyte colony-stimulating factor; GM-CSF: Granulocyte-macrophage colony-stimulating factor; IFN γ : Interferon- γ ; IL: Interleukin; IP: Interferon-induced protein; LTP: Long-term potentiation; MCP-1: Monocyte chemotactic protein-1; MIP-1 β : Macrophage inflammatory protein-1 β ; PC: Principal components; PCA: Principal component analysis; RANTES: Regulated upon activation normal T cell expressed and secreted factor; ROC: Receiver operating characteristic; TMA: Trimethylamine; TMAO: Trimethylamine-N-oxide; TNF: Tumor necrosis factor; WT: Wild type.

AUTHOR CONTRIBUTIONS

YZ and RW conceived of the study and participated in its design and coordination and helped to draft the manuscript. XW carried out behavioral tests, biochemical and histochemical analyses, and wrote and revised the manuscript; QW and YS participated in the design of the study, wrote and revised the manuscript. SF participated in the multiplex bead analysis. SF and XZ participated in the histochemical analyses. All authors read and approved the final manuscript.

CONFLICTS OF INTEREST

The authors declare that they have no conflicts of interests.

FUNDING

This work was supported by grants from the Natural Science Foundation of Heilongjiang Province of China

(No. ZD2017017), the Harbin Special Fund for Scientific and Technological Innovation Talents (No. 2016RAXYJ073), and the Science Foundation of Heilongjiang Academy of Medical Science (No. 201811).

REFERENCES

1. Steel N, Ford JA, Newton JN, Davis AC, Vos T, Naghavi M, Glenn S, Hughes A, Dalton AM, Stockton D, Humphreys C, Dallat M, Schmidt J, et al. Changes in health in the countries of the UK and 150 English Local Authority areas 1990-2016: a systematic analysis for the Global Burden of Disease Study 2016. *Lancet*. 2018; 392:1647–61. [https://doi.org/10.1016/S0140-6736\(18\)32207-4](https://doi.org/10.1016/S0140-6736(18)32207-4) PMID:[30497795](https://pubmed.ncbi.nlm.nih.gov/30497795/)
2. Shan W, Li J, Xu W, Li H, Zuo Z. Critical role of UQCRC1 in embryo survival, brain ischemic tolerance and normal cognition in mice. *Cell Mol Life Sci*. 2019; 76:1381–1396. <https://doi.org/10.1007/s00018-019-03007-6> PMID:[30666338](https://pubmed.ncbi.nlm.nih.gov/30666338/)
3. Fung TC, Olson CA, Hsiao EY. Interactions between the microbiota, immune and nervous systems in health and disease. *Nat Neurosci*. 2017; 20:145–155. <https://doi.org/10.1038/nn.4476> PMID:[28092661](https://pubmed.ncbi.nlm.nih.gov/28092661/)
4. Wu SC, Cao ZS, Chang KM, Juang JL. Intestinal microbial dysbiosis aggravates the progression of Alzheimer's disease in *Drosophila*. *Nat Commun*. 2017; 8:24. <https://doi.org/10.1038/s41467-017-00040-6> PMID:[28634323](https://pubmed.ncbi.nlm.nih.gov/28634323/)
5. Xu R, Wang Q. Towards understanding brain-gut-microbiome connections in Alzheimer's disease. *BMC Syst Biol*. 2016; 10:63. <https://doi.org/10.1186/s12918-016-0307-y> PMID:[27585440](https://pubmed.ncbi.nlm.nih.gov/27585440/)
6. Vogt NM, Romano KA, Darst BF, Engelman CD, Johnson SC, Carlsson CM, Asthana S, Blennow K, Zetterberg H, Bendlin BB, Rey FE. The gut microbiota-derived metabolite trimethylamine N-oxide is elevated in Alzheimer's disease. *Alzheimers Res Ther*. 2018; 10:124. <https://doi.org/10.1186/s13195-018-0451-2> PMID:[30579367](https://pubmed.ncbi.nlm.nih.gov/30579367/)
7. Zhu W, Gregory JC, Org E, Buffa JA, Gupta N, Wang Z, Li L, Fu X, Wu Y, Mehrabian M, Sartor RB, McIntyre TM, Silverstein RL, et al. Gut Microbial Metabolite TMAO Enhances Platelet Hyperreactivity and Thrombosis Risk. *Cell*. 2016; 165:111–24. <https://doi.org/10.1016/j.cell.2016.02.011> PMID:[26972052](https://pubmed.ncbi.nlm.nih.gov/26972052/)
8. Koeth RA, Wang Z, Levison BS, Buffa JA, Org E, Sheehy BT, Britt EB, Fu X, Wu Y, Li L, Smith JD, DiDonato JA, Chen J, et al. Intestinal microbiota metabolism of L-carnitine, a nutrient in red meat, promotes atherosclerosis. *Nat Med*. 2013; 19:576–85. <https://doi.org/10.1038/nm.3145> PMID:[23563705](https://pubmed.ncbi.nlm.nih.gov/23563705/)
9. Tilg H. A Gut Feeling about Thrombosis. *N Engl J Med*. 2016; 374:2494–96. <https://doi.org/10.1056/NEJMcibr1604458> PMID:[27332910](https://pubmed.ncbi.nlm.nih.gov/27332910/)
10. Akbari E, Asemi Z, Daneshvar Kakhaki R, Bahmani F, Kouchaki E, Tamtaji OR, Hamidi GA, Salami M. Effect of Probiotic Supplementation on cognitive function and metabolic status in Alzheimer's disease: a randomized, double-blind and controlled trial. *Front Aging Neurosci*. 2016; 8:256. <https://doi.org/10.3389/fnagi.2016.00256> PMID:[27891089](https://pubmed.ncbi.nlm.nih.gov/27891089/)
11. Athari Nik Azm S, Djazayeri A, Safa M, Azami K, Ahmadvand B, Sabbaghziarani F, Sharifzadeh M, Vafa M. Lactobacilli and bifidobacteria ameliorate memory and learning deficits and oxidative stress in β -amyloid (1-42) injected rats. *Appl Physiol Nutr Metab*. 2018; 43:718–726. <https://doi.org/10.1139/apnm-2017-0648> PMID:[29462572](https://pubmed.ncbi.nlm.nih.gov/29462572/)
12. Akison LK, Kuo J, Reid N, Boyd RN, Moritz KM. Effect of choline supplementation on neurological, cognitive, and behavioral outcomes in offspring arising from alcohol exposure during development: a quantitative systematic review of clinical and preclinical studies. *Alcohol Clin Exp Res*. 2018; 42:1591–611. <https://doi.org/10.1111/acer.13817> PMID:[29928762](https://pubmed.ncbi.nlm.nih.gov/29928762/)
13. Edwards CG, Walk AM, Cannavale CN, Flemming IR, Thompson SV, Reeser GR, Holscher HD, Khan NA. Dietary choline is related to neural efficiency during a selective attention task among middle-aged adults with overweight and obesity. *Nutr Neurosci*. 2019; 1–10. [Epub ahead of print]. <https://doi.org/10.1080/1028415X.2019.1623456> PMID:[31156061](https://pubmed.ncbi.nlm.nih.gov/31156061/)
14. Swets JA. Measuring the accuracy of diagnostic systems. *Science*. 1988; 240:1285–93. <https://doi.org/10.1126/science.3287615> PMID:[3287615](https://pubmed.ncbi.nlm.nih.gov/3287615/)
15. Kalagi NA, Abbott KA, Alburikan KA, Alkofide HA, Stojanovski E, Garg ML. Modulation of circulating trimethylamine N-Oxide concentrations by dietary supplements and pharmacological agents: A systematic review. *Adv Nutr*. 2019; 10:876–887. <https://doi.org/10.1093/advances/nmz012> PMID:[31073588](https://pubmed.ncbi.nlm.nih.gov/31073588/)
16. Tao L, Wang B, Zhong Y, Pow SH, Zeng X, Qin C, Zhang P, Chen S, He W, Tan Y, Liu H, Jiang Y, Chen W, Chen

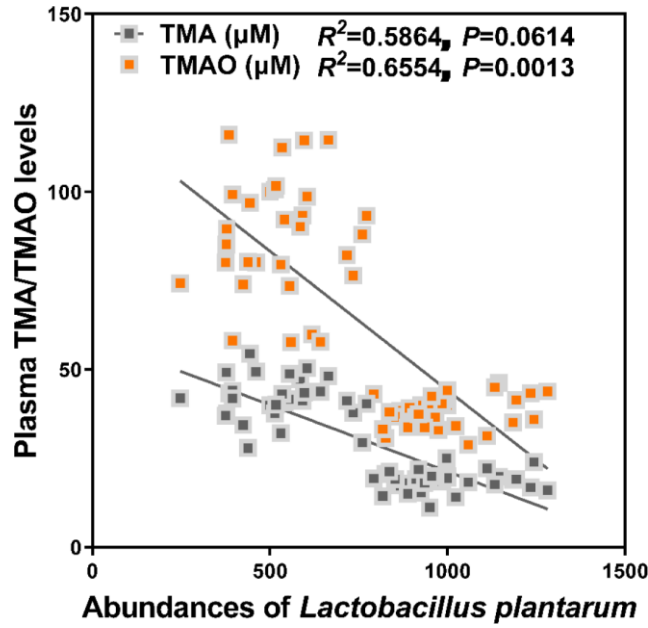
- YZ. Database and Bioinformatics studies of probiotics. *J Agric Food Chem*. 2017; 65:7599–606.
<https://doi.org/10.1021/acs.jafc.7b01815>
 PMID:[28727425](https://pubmed.ncbi.nlm.nih.gov/28727425/)
17. Cooke SF, Bear MF. Stimulus-selective response plasticity in the visual cortex: an assay for the assessment of pathophysiology and treatment of cognitive impairment associated with psychiatric disorders. *Biol Psychiatry*. 2012; 71:487–95.
<https://doi.org/10.1016/j.biopsych.2011.09.006>
 PMID:[22019003](https://pubmed.ncbi.nlm.nih.gov/22019003/)
 18. Donner L, Fälker K, Gremer L, Klinker S, Pagani G, Ljungberg LU, Lothmann K, Rizzi F, Schaller M, Gohlke H, Willbold D, Grenegard M, Elvers M. Platelets contribute to amyloid- β aggregation in cerebral vessels through integrin α IIb β 3-induced outside-in signaling and clusterin release. *Sci Signal*. 2016; 9:ra52.
<https://doi.org/10.1126/scisignal.aaf6240>
 PMID:[27221710](https://pubmed.ncbi.nlm.nih.gov/27221710/)
 19. Foster EM, Dangla-Valls A, Lovestone S, Ribe EM, Buckley NJ. Clusterin in Alzheimer's disease: mechanisms, genetics, and lessons from other pathologies. *Front Neurosci*. 2019; 13:164.
<https://doi.org/10.3389/fnins.2019.00164>
 PMID:[30872998](https://pubmed.ncbi.nlm.nih.gov/30872998/)
 20. Yang DS, Yip CM, Huang TH, Chakrabartty A, Fraser PE. Manipulating the amyloid-beta aggregation pathway with chemical chaperones. *J Biol Chem*. 1999; 274:32970–74.
<https://doi.org/10.1074/jbc.274.46.32970>
 PMID:[10551864](https://pubmed.ncbi.nlm.nih.gov/10551864/)
 21. Meng F, Li N, Li D, Song B, Li L. The presence of elevated circulating trimethylamine N-oxide exaggerates postoperative cognitive dysfunction in aged rats. *Behav Brain Res*. 2019; 368:111902.
<https://doi.org/10.1016/j.bbr.2019.111902>
 PMID:[30980850](https://pubmed.ncbi.nlm.nih.gov/30980850/)
 22. Li D, Ke Y, Zhan R, Liu C, Zhao M, Zeng A, Shi X, Ji L, Cheng S, Pan B, Zheng L, Hong H. Trimethylamine-N-oxide promotes brain aging and cognitive impairment in mice. *Aging Cell*. 2018; 17:e12768.
<https://doi.org/10.1111/acer.12768> PMID:[29749694](https://pubmed.ncbi.nlm.nih.gov/29749694/)
 23. Cryan JF, Dinan TG. Mind-altering microorganisms: the impact of the gut microbiota on brain and behaviour. *Nat Rev Neurosci*. 2012; 13:701–12.
<https://doi.org/10.1038/nrn3346> PMID:[22968153](https://pubmed.ncbi.nlm.nih.gov/22968153/)
 24. Lyte M. Microbial endocrinology: host-microbiota neuroendocrine interactions influencing brain and behavior. *Gut Microbes*. 2014; 5:381–89.
<https://doi.org/10.4161/gmic.28682> PMID:[24690573](https://pubmed.ncbi.nlm.nih.gov/24690573/)
 25. Sharon G, Sampson TR, Geschwind DH, Mazmanian SK. The central nervous system and the Gut microbiome. *Cell*. 2016; 167:915–32.
<https://doi.org/10.1016/j.cell.2016.10.027>
 PMID:[27814521](https://pubmed.ncbi.nlm.nih.gov/27814521/)
 26. Vogt NM, Kerby RL, Dill-McFarland KA, Harding SJ, Merluzzi AP, Johnson SC, Carlsson CM, Asthana S, Zetterberg H, Blennow K, Bendlin BB, Rey FE. Gut microbiome alterations in Alzheimer's disease. *Sci Rep*. 2017; 7:13537.
<https://doi.org/10.1038/s41598-017-13601-y>
 PMID:[29051531](https://pubmed.ncbi.nlm.nih.gov/29051531/)
 27. Leblhuber F, Geisler S, Steiner K, Fuchs D, Schütz B. Elevated fecal calprotectin in patients with Alzheimer's dementia indicates leaky gut. *J Neural Transm (Vienna)*. 2015; 122:1319–22.
<https://doi.org/10.1007/s00702-015-1381-9>
 PMID:[25680441](https://pubmed.ncbi.nlm.nih.gov/25680441/)
 28. Shen L, Liu L, Ji HF. Alzheimer's disease histological and behavioral manifestations in transgenic mice correlate with specific gut microbiome state. *J Alzheimers Dis*. 2017; 56:385–90.
<https://doi.org/10.3233/JAD-160884> PMID:[27911317](https://pubmed.ncbi.nlm.nih.gov/27911317/)
 29. Harach T, Marungruang N, Duthilleul N, Cheatham V, Mc Coy KD, Frisoni G, Neher JJ, Fåk F, Jucker M, Lasser T, Bolmont T. Reduction of Abeta amyloid pathology in APPPS1 transgenic mice in the absence of gut microbiota. *Sci Rep*. 2017; 7:41802.
<https://doi.org/10.1038/srep41802> PMID:[28176819](https://pubmed.ncbi.nlm.nih.gov/28176819/)
 30. Grant MC, Baker JS. An overview of the effect of probiotics and exercise on mood and associated health conditions. *Crit Rev Food Sci Nutr*. 2017; 57:3887–93.
<https://doi.org/10.1080/10408398.2016.1189872>
 PMID:[27246320](https://pubmed.ncbi.nlm.nih.gov/27246320/)
 31. He B, Hoang TK, Wang T, Ferris M, Taylor CM, Tian X, Luo M, Tran DQ, Zhou J, Tatevian N, Luo F, Molina JG, Blackburn MR, et al. Resetting microbiota by *Lactobacillus reuteri* inhibits T reg deficiency-induced autoimmunity via adenosine A2A receptors. *J Exp Med*. 2017; 214:107–23.
<https://doi.org/10.1084/jem.20160961>
 PMID:[27994068](https://pubmed.ncbi.nlm.nih.gov/27994068/)
 32. O'Shea EF, Cotter PD, Stanton C, Ross RP, Hill C. Production of bioactive substances by intestinal bacteria as a basis for explaining probiotic mechanisms: bacteriocins and conjugated linoleic acid. *Int J Food Microbiol*. 2012; 152:189–205.
<https://doi.org/10.1016/j.ijfoodmicro.2011.05.025>
 PMID:[21742394](https://pubmed.ncbi.nlm.nih.gov/21742394/)
 33. Ventura M, O'Flaherty S, Claesson MJ, Turrone F, Klaenhammer TR, van Sinderen D, O'Toole PW. Genome-scale analyses of health-promoting bacteria: probiogenomics. *Nat Rev Microbiol*. 2009; 7:61–71.
<https://doi.org/10.1038/nrmicro2047> PMID:[19029955](https://pubmed.ncbi.nlm.nih.gov/19029955/)

34. Choi HJ, Lee NK, Paik HD. Health benefits of lactic acid bacteria isolated from kimchi, with respect to immunomodulatory effects. *Food Sci Biotechnol*. 2015; 24:783–89. <https://doi.org/10.1007/s10068-015-0102-3>
35. Tillisch K, Labus J, Kilpatrick L, Jiang Z, Stains J, Ebrat B, Guyonnet D, Legrain-Raspaud S, Trotin B, Naliboff B, Mayer EA. Consumption of fermented milk product with probiotic modulates brain activity. *Gastroenterology*. 2013; 144:1394–401, 1401.e1-4. <https://doi.org/10.1053/j.gastro.2013.02.043> PMID:23474283
36. Ohland CL, Kish L, Bell H, Thiesen A, Hotte N, Pankiv E, Madsen KL. Effects of *Lactobacillus helveticus* on murine behavior are dependent on diet and genotype and correlate with alterations in the gut microbiome. *Psychoneuroendocrinology*. 2013; 38:1738–47. <https://doi.org/10.1016/j.psyneuen.2013.02.008> PMID:23566632
37. Davari S, Talaei SA, Alaei H, Salami M. Probiotics treatment improves diabetes-induced impairment of synaptic activity and cognitive function: behavioral and electrophysiological proofs for microbiome-gut-brain axis. *Neuroscience*. 2013; 240:287–96. <https://doi.org/10.1016/j.neuroscience.2013.02.055> PMID:23500100
38. Gareau MG, Wine E, Rodrigues DM, Cho JH, Whary MT, Philpott DJ, Macqueen G, Sherman PM. Bacterial infection causes stress-induced memory dysfunction in mice. *Gut*. 2011; 60:307–17. <https://doi.org/10.1136/gut.2009.202515> PMID:20966022
39. Distrutti E, O'Reilly JA, McDonald C, Cipriani S, Renga B, Lynch MA, Fiorucci S. Modulation of intestinal microbiota by the probiotic VSL#3 resets brain gene expression and ameliorates the age-related deficit in LTP. *PLoS One*. 2014; 9:e106503. <https://doi.org/10.1371/journal.pone.0106503> PMID:25202975
40. Obeid R, Awwad HM, Keller M, Geisel J. Trimethylamine-N-oxide and its biological variations in vegetarians. *Eur J Nutr*. 2017; 56:2599–609. <https://doi.org/10.1007/s00394-016-1295-9> PMID:27562778
41. Wang Z, Bergeron N, Levison BS, Li XS, Chiu S, Jia X, Koeth RA, Li L, Wu Y, Tang WH, Krauss RM, Hazen SL. Impact of chronic dietary red meat, white meat, or non-meat protein on trimethylamine N-oxide metabolism and renal excretion in healthy men and women. *Eur Heart J*. 2019; 40:583–94. <https://doi.org/10.1093/eurheartj/ehy799> PMID:30535398
42. Ufnal M, Zadlo A, Ostaszewski R. TMAO: A small molecule of great expectations. *Nutrition*. 2015; 31:1317–23. <https://doi.org/10.1016/j.nut.2015.05.006> PMID:26283574
43. Boini KM, Hussain T, Li PL, Koka S. Trimethylamine-N-Oxide Instigates NLRP3 Inflammasome Activation and Endothelial Dysfunction. *Cell Physiol Biochem*. 2017; 44:152–162. <https://doi.org/10.1159/000484623> PMID:29130962
44. Li T, Chen Y, Gua C, Li X. Elevated Circulating Trimethylamine N-Oxide Levels Contribute to Endothelial Dysfunction in Aged Rats through Vascular Inflammation and Oxidative Stress. *Front Physiol*. 2017; 8:350. <https://doi.org/10.3389/fphys.2017.00350> PMID:28611682
45. Yerbury JJ, Wilson MR. Extracellular chaperones modulate the effects of Alzheimer's patient cerebrospinal fluid on Abeta(1-42) toxicity and uptake. *Cell Stress Chaperones*. 2010; 15:115–21. <https://doi.org/10.1007/s12192-009-0122-0> PMID:19472074
46. Yu JT, Ma XY, Wang YL, Sun L, Tan L, Hu N, Tan L. Genetic variation in clusterin gene and Alzheimer's disease risk in Han Chinese. *Neurobiol Aging*. 2013; 34:1921.e17-23. <https://doi.org/10.1016/j.neurobiolaging.2013.01.010> PMID:23411014
47. Carrasquillo MM, Belbin O, Hunter TA, Ma L, Bisceglia GD, Zou F, Crook JE, Pankratz VS, Dickson DW, Graff-Radford NR, Petersen RC, Morgan K, Younkin SG. Replication of CLU, CR1, and PICALM associations with alzheimer disease. *Arch Neurol*. 2010; 67:961–4. <https://doi.org/10.1001/archneurol.2010.147> PMID:20554627
48. Yerbury JJ, Poon S, Meehan S, Thompson B, Kumita JR, Dobson CM, Wilson MR. The extracellular chaperone clusterin influences amyloid formation and toxicity by interacting with prefibrillar structures. *FASEB J*. 2007; 21:2312–22. <https://doi.org/10.1096/fj.06-7986com> PMID:17412999
49. Narayan P, Holmström KM, Kim DH, Whitcomb DJ, Wilson MR, St George-Hyslop P, Wood NW, Dobson CM, Cho K, Abramov AY, Klenerman D. Rare individual amyloid- β oligomers act on astrocytes to initiate neuronal damage. *Biochemistry*. 2014; 53:2442–53. <https://doi.org/10.1021/bi401606f> PMID:24717093
50. DeMattos RB, O'dell MA, Parsadanian M, Taylor JW, Harmony JA, Bales KR, Paul SM, Aronow BJ, Holtzman DM. Clusterin promotes amyloid plaque formation and is critical for neuritic toxicity in a mouse model of

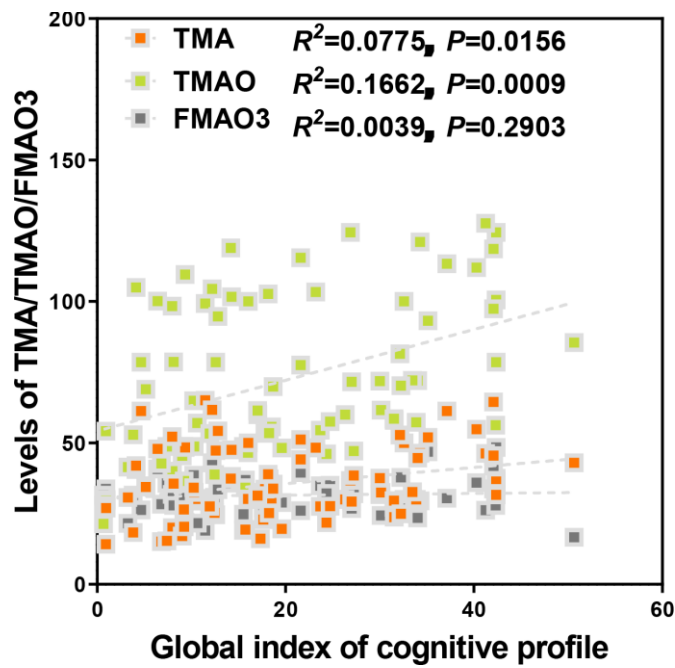
- Alzheimer's disease. *Proc Natl Acad Sci USA*. 2002; 99:10843–48.
<https://doi.org/10.1073/pnas.162228299>
PMID:[12145324](https://pubmed.ncbi.nlm.nih.gov/12145324/)
51. Wojtas AM, Kang SS, Olley BM, Gatherer M, Shinohara M, Lozano PA, Liu CC, Kurti A, Baker KE, Dickson DW, Yue M, Petrucelli L, Bu G, et al. Loss of clusterin shifts amyloid deposition to the cerebrovasculature via disruption of perivascular drainage pathways. *Proc Natl Acad Sci USA*. 2017; 114:E6962–71.
<https://doi.org/10.1073/pnas.1701137114>
PMID:[28701379](https://pubmed.ncbi.nlm.nih.gov/28701379/)
52. Sims R, van der Lee SJ, Naj AC, Bellenguez C, Badarinarayan N, Jakobsdottir J, Kunkle BW, Boland A, Raybould R, Bis JC, Martin ER, Grenier-Boley B, Heilmann-Heimbach S, et al, and ARUK Consortium, and GERAD/PERADES, CHARGE, ADGC, EADI. Rare coding variants in PLCG2, ABI3, and TREM2 implicate microglial-mediated innate immunity in Alzheimer's disease. *Nat Genet*. 2017; 49:1373–84.
<https://doi.org/10.1038/ng.3916> PMID:[28714976](https://pubmed.ncbi.nlm.nih.gov/28714976/)
53. Guerreiro R, Wojtas A, Bras J, Carrasquillo M, Rogeava E, Majounie E, Cruchaga C, Sassi C, Kauwe JS, Younkin S, Hazrati L, Collinge J, Pocock J, et al, and Alzheimer Genetic Analysis Group. TREM2 variants in Alzheimer's disease. *N Engl J Med*. 2013; 368:117–27.
<https://doi.org/10.1056/NEJMoa1211851>
PMID:[23150934](https://pubmed.ncbi.nlm.nih.gov/23150934/)
54. Shim YJ, Kang BH, Choi BK, Park IS, Min BH. Clusterin induces the secretion of TNF- α and the chemotactic migration of macrophages. *Biochem Biophys Res Commun*. 2012; 422:200–05.
<https://doi.org/10.1016/j.bbrc.2012.04.162>
PMID:[22575505](https://pubmed.ncbi.nlm.nih.gov/22575505/)
55. Sonn CH, Yu YB, Hong YJ, Shim YJ, Bluestone JA, Min BH, Lee KM. Clusterin synergizes with IL-2 for the expansion and IFN- γ production of natural killer cells. *J Leukoc Biol*. 2010; 88:955–63.
<https://doi.org/10.1189/jlb.0310157>
PMID:[20729304](https://pubmed.ncbi.nlm.nih.gov/20729304/)
56. de Retana SF, Marazuela P, Solé M, Colell G, Bonaterra A, Sánchez-Quesada JL, Montaner J, MasPOCH D, Cano-Sarabia M, Hernández-Guillamon M. Peripheral administration of human recombinant ApoJ/clusterin modulates brain beta-amyloid levels in APP23 mice. *Alzheimers Res Ther*. 2019; 11:42.
<https://doi.org/10.1186/s13195-019-0498-8>
PMID:[31077261](https://pubmed.ncbi.nlm.nih.gov/31077261/)
57. Jenne DE, Tschopp J. Molecular structure and functional characterization of a human complement cytotoxicity inhibitor found in blood and seminal plasma: identity to sulfated glycoprotein 2, a constituent of rat testis fluid. *Proc Natl Acad Sci USA*. 1989; 86:7123–27.
<https://doi.org/10.1073/pnas.86.18.7123>
PMID:[2780565](https://pubmed.ncbi.nlm.nih.gov/2780565/)
58. Bai C, Biwersi J, Verkman AS, Matthay MA. A mouse model to test the in vivo efficacy of chemical chaperones. *J Pharmacol Toxicol Methods*. 1998; 40:39–45.
[https://doi.org/10.1016/S1056-8719\(98\)00034-3](https://doi.org/10.1016/S1056-8719(98)00034-3)
PMID:[9920533](https://pubmed.ncbi.nlm.nih.gov/9920533/)
59. Mello CC, Barrick D. Measuring the stability of partly folded proteins using TMAO. *Protein Sci*. 2003; 12:1522–9.
<https://doi.org/10.1110/ps.0372903>
PMID:[12824497](https://pubmed.ncbi.nlm.nih.gov/12824497/)
60. Bennett BJ, de Aguiar Vallim TQ, Wang Z, Shih DM, Meng Y, Gregory J, Allayee H, Lee R, Graham M, Crooke R, Edwards PA, Hazen SL, Lusis AJ. Trimethylamine-N-oxide, a metabolite associated with atherosclerosis, exhibits complex genetic and dietary regulation. *Cell Metab*. 2013; 17:49–60.
<https://doi.org/10.1016/j.cmet.2012.12.011>
PMID:[23312283](https://pubmed.ncbi.nlm.nih.gov/23312283/)
61. Li D, Liu CM, Luo R, Sadakane K, Lam TW. MEGAHIT: an ultra-fast single-node solution for large and complex metagenomics assembly via succinct de Bruijn graph. *Bioinformatics*. 2015; 31:1674–76.
<https://doi.org/10.1093/bioinformatics/btv033>
PMID:[25609793](https://pubmed.ncbi.nlm.nih.gov/25609793/)
62. Noguchi H, Park J, Takagi T. MetaGene: prokaryotic gene finding from environmental genome shotgun sequences. *Nucleic Acids Res*. 2006; 34:5623–30.
<https://doi.org/10.1093/nar/gkl723> PMID:[17028096](https://pubmed.ncbi.nlm.nih.gov/17028096/)
63. Fu L, Niu B, Zhu Z, Wu S, Li W. CD-HIT: accelerated for clustering the next-generation sequencing data. *Bioinformatics*. 2012; 28:3150–52.
<https://doi.org/10.1093/bioinformatics/bts565>
PMID:[23060610](https://pubmed.ncbi.nlm.nih.gov/23060610/)
64. Li R, Li Y, Kristiansen K, Wang J. SOAP: short oligonucleotide alignment program. *Bioinformatics*. 2008; 24:713–14.
<https://doi.org/10.1093/bioinformatics/btn025>
PMID:[18227114](https://pubmed.ncbi.nlm.nih.gov/18227114/)
65. Altschul SF, Madden TL, Schäffer AA, Zhang J, Zhang Z, Miller W, Lipman DJ. Gapped BLAST and PSI-BLAST: a new generation of protein database search programs. *Nucleic Acids Res*. 1997; 25:3389–402.
<https://doi.org/10.1093/nar/25.17.3389>
PMID:[9254694](https://pubmed.ncbi.nlm.nih.gov/9254694/)

SUPPLEMENTARY MATERIALS

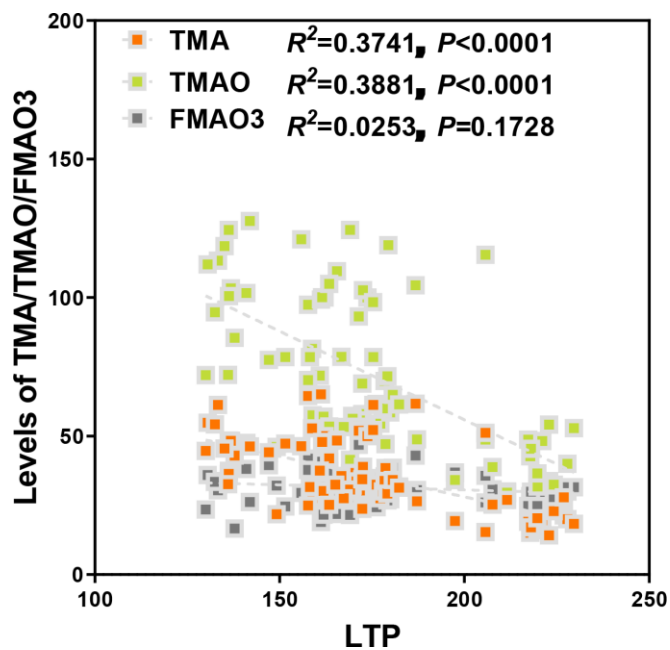
Supplementary Figures



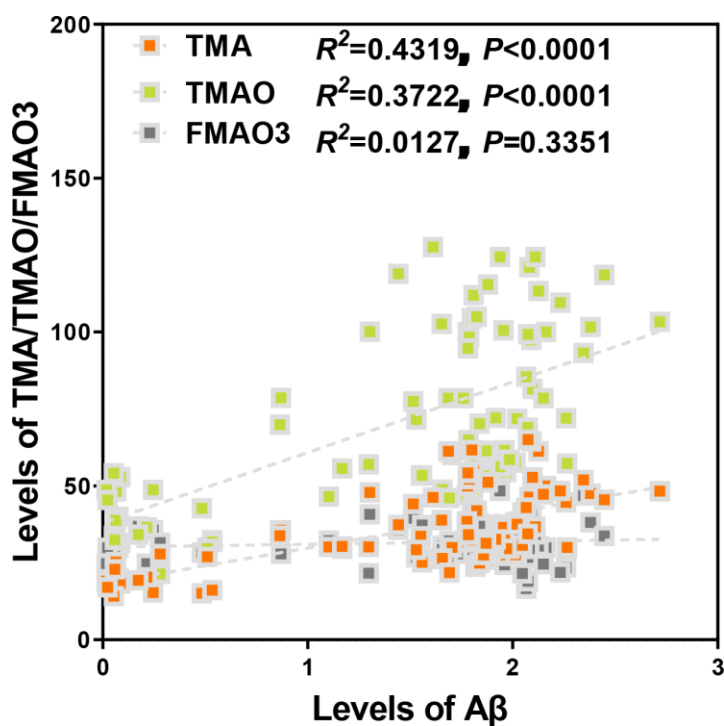
Supplementary Figure 1. Pearson correlation between the relative abundances of *L. plantarum* and plasma TMA and TMAO concentrations from mice grouped by dietary status (chow and choline). n=60.



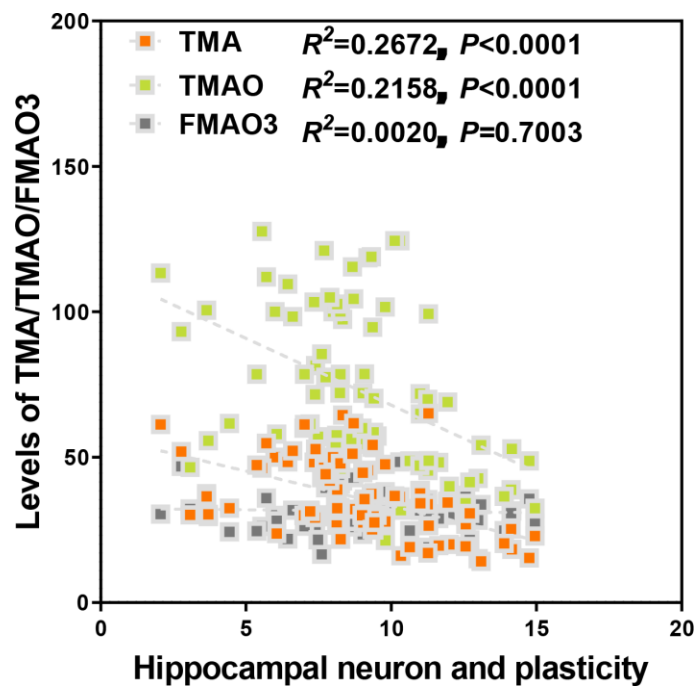
Supplementary Figure 2. Spearman correlation between the TMA/TMAO/FMAO3 concentrations and cognitive impairments in WT and APP/PS1 mice. n=75.



Supplementary Figure 3. Spearman correlation between the TMA/TMAO/FMAO3 concentrations and LTP in WT and APP/PS1 mice. LTP means long-term potentiation. n=75.



Supplementary Figure 4. Spearman correlation between the TMA/TMAO/FMAO3 concentrations and A β deterioration in the hippocampus of WT and APP/PS1 mice. n=75.



Supplementary Figure 5. Spearman correlation between the TMA/TMAO/FMAO3 concentrations and hippocampal neuron and plasticity deterioration in the hippocampus of WT and APP/PS1 mice. n=75.